Soft Matter

Accepted Manuscript

ROYAL SOCIETY OF CHEMISTRY

www.rsc.org/softmatter

Soft Matter

FULL PAPER SUBMISSION

Where physics meets chemistry meets biology for fundamental soft matter research

2012 Impact factor: **3.91** 2012 Immediacy index: **1.01** www.rsc.org/softmatter

Soft Matter has a global circulation and interdisciplinary audience with a particular focus on the interface between physics, biology, chemical engineering, materials science and chemistry.

The following paper has been submitted to *Soft Matter* for consideration as a **full paper**.

Soft Matter aims to publish **high quality** papers reporting on the generic science underpinning the properties, applications, and phenomena of soft matter. The primary criterion for acceptance of a contribution for publication is that it must report high-quality new science and make a significant contribution to its field. *Soft Matter* is an **interdisciplinary** journal and suitable papers should cross disciplines or be highly significant within the field from which they originate.

Routine or incremental work, however competently researched and reported, should not be recommended for publication if it does not meet our expectations with regard to novelty and impact.

Thank you for your effort in reviewing this submission. It is only through the continued service of referees that we can maintain both the high quality of the publication and the rapid response times to authors.

We would greatly appreciate if you could review this paper in **two weeks**. Please let us know if that will not be possible. Please support all comments with scientific justifications or we may be unable to use your report/ask for extra feedback.

Once again, we appreciate your time in serving as a reviewer. To acknowledge this, the RSC offers a **25% discount** on its books: http://www.rsc.org/Shop/books/discounts.asp. Please also consider submitting your next manuscript to *Soft Matter*.

Best wishes,

Liz Dunn

Liz Dunn, Editor, *Soft Matter*

BASF
The Chemical Company

To the editor of the RSC journal ***Soft Matter***

May 20, 2014
Horst Hintze-Bruening
Global Applied Research
Tel. +492501142007
Fax +49250114712007
horst.hintze-bruening@basf.com

Submission to Soft Matter

Dear Editor,

It is our pleasure to submit our manuscript as an article for *Soft Matter* entitled

"Ordered Liquids and Hydrogels from Alkenyl Succinic Ester Terminated Bola-Amphiphiles for Large-Scale Applications" from Thomas Lohmeier, Michael Bredol, Eduard Schreiner and Horst Hintze-Bruening.

The study is devoted to new materials concepts for the formulation of anisotropic organic films, e.g. coatings with improved property profiles with regard to mechanical impact resistance, diffusion barrier or orientation of macroscopic 2D effect pigments. Leaving self-stratification and tedious application methods like the layer-by-layer technique aside such anisotropic films are still economically difficult to realize for large scale applications, e.g. industrial coatings.

Our approach ties up to our previously published work which made use of 2D particle based ordered liquids (*Soft Matter*, 2011, **7**, 4242) and describes the self-assembly of bola-amphiphilic systems in the aqueous phase to form ordered liquids and hydrogels respectively. With regard to large-scale applications the emphasis is put on polymeric, ill-defined systems which are based on inexpensive, partly renewable raw materials making use of a – to the best of our knowledge – novel bola motif consisting of alkenyl succinic ester head groups.

By using low angle X-ray scattering, ^{2}H-NMR, optical and cryo-microscopy (AFM, TEM) as well as rheological methods we have shown how molecular plurality translates into ordered, anisotropic mesophases and that molecular simulation on monomeric systems is corroborating the experiments.

Since the described systems are based on affordable, unobjectionable raw materials and economical and scalable manufacturing processes they certainly will spur further technical improvements in the sustainable development of large-scale applications not restricted to organic coatings, e.g. adhesives, films and membranes or colloidal products relying on distinct hydrogel properties.

Best regards,

Sitz der Gesellschaft:
BASF Coatings GmbH
Glasuritstrasse 1
D-48165 Münster

Telefon: +49 2501 14-0
Telefax: +49 2501 14-33 73

Registergericht:
Amtsgericht Münster

Eintragungsnummer:
HRB 5144

Geschäftsführung:
Dr. Markus Kamieth (Vorsitzender),
Eva Müller

Umsatzsteueridentifikationsnummer:
DE811122710

Journal Name

RSCPublishing

ARTICLE

Ordered Liquids and Hydrogels from Alkenyl Succinic Ester Terminated Bola-Amphiphiles for Large-Scale Applications

Cite this: DOI: 10.1039/x0xx00000x

Received 00th January 2012,
Accepted 00th January 2012

DOI: 10.1039/x0xx00000x

www.rsc.org/

Thomas Lohmeier,[a] Michael Bredol,[b] Eduard Schreiner[c] and Horst Hintze-Bruening*[a]

The present study describes an economic and scalable approach to aqueous mesophases from bola-amphiphiles (BA) obtained via nucleophilic addition of dimer fatty acid based α,ω-polyesterdiols (PES) on cyclic acid anhydrides and conversion of the carboxylic end groups into ammonium salts. Novel bola-amphiphilic head groups are introduced using alkenyl succinic anhydrides (ASA). The additional terminal hydrophobic side chains favour the self-assembly of polymeric BA of different molecular weights into nanoscale anisotropic objects, their shape and ordering into nematic or lamellar-like phases being dependent on the length and structural uniformity of the ASA chains. Corresponding diester based on C15 (hydrogenated bisphenol-A, HBA) and C8 (1,4-cyclohexanedimethanol, CHDM) spacer have been prepared and the self-assembly of the resulting BA in water has been studied using SAXS, ^{2}H-NMR and optical polarization microscopy. While the rigid C8 spacer impedes any ordering, ASA capped C15 tend to form ordered hydrogels over extended regions of the phase diagram that resemble mesh phases and L_α/L_3 polymorphism. Rheological and simulation results confirm the presence of elastically responding bicontinuous morphologies respectively biased porous assemblies resembling interconnected mesh phases. Both the use of dimer fatty acid based spacer as well as of ASA head groups open up large-scale applications of ordered liquids (or hydrogels) as a formulation basis for e.g. films, coatings and adhesives.

Introduction

Self-assembly of amphiphiles is a convenient strategy to obtain functional nanostructures useful as soft templates for the fabrication of (porous) solids,[1] for the encapsulation of actives or food additives[2] or for advanced applications like optoelectronics.[3] Although numerous examples for thin films that are anisotropic on the mesoscale are known,[4] in the context of large scale applications like organic coatings for automotives or aviation the use of ordered materials for mesoscopical, anisotropic layers has barely been reported. However attractive property profiles, e.g. combined mechanical reinforcement, diffusion barrier and pigment orientation might be realized making use of a lyotropic mesophase as an intermediate step of the formulation as we have shown recently: in the presence of a polyester dispersion individual platelets of a layered double hydroxide adopt a nematic like ordering in the aqueous phase.[5] However the limited extension of nematically arranged platelets perpendicular to the director led to a superimposed lamellar assembly on larger length scales which was transferred into the solid coating in the form of an ordered array of polymer intercalated platelets. In this study we describe an approach to obtain lyotropic ordering of polymeric bola-amphiphiles in the aqueous phase, namely extended layered structures, thus mimicking robust lipid membranes of archaebacteria that consist of bola-amphiphiles, a sort of amphiphiles comprising two hydrophilic heads connected by a hydrophobic spacer.

Since early studies on bola electrolytes[6] and on cationic bola-form detergents[7] as well as the pioneering investigations of Vittorio Luzzati on the polymorphism of several extracted archae-bacterial bola-amphiphiles[8] numerous synthetic systems have been prepared and their self-assembly studied,[9] the main aspects investigated being the nature of the head groups (non-, an- or cationic) and the spacer (aliphatic, aromatic, fluorinated), the molecular architecture (symmetry, length, bulkiness, shape) or the concept of supra-amphiphiles featuring specific binding sites and the role of the counter ion.[10] Common to all is the molecular uniformity (purity) of the organic mesogen resulting from tedious synthesis and purification procedures that are economically not affordable for large-scale industrial application. Furthermore low molecular weights and thus high proportions of hydrophilic, possibly ionic groups are incompatible with coating applications which are thought to provide resistance against humidity with regard to swelling and (ion) permeability.

We found that ill-defined bola-form polyesters prepared from inexpensive raw materials self-assemble in aqueous solutions into ordered structures and could thus overcome the economic and technological constraints. Besides hydrophobicity stemming from dimer fatty acids in the polymer backbone we have investigated the effect of hydrophobic aliphatic side groups in α- and β-position to the ionic head group on the self-assembly. The role of mono- versus of double-stranded bolaform architecture has already been addressed in the context of vesicle formation of symmetrical glycosylated bola-amphiphiles[11] making reference to similar asymmetric molecules where hydrophobic chains were attached at the anomeric site of the head groups' furanose ring.[12] In the present study the head groups result from nucleophilic addition of an α,ω-polyesterdiol (PES) on alkenyl succinic anhydrides (ASA) which have been proposed for numerous technical applications and are used on large scale, e.g. as sizing agents for starch[13] and cellulose[14] in the food and paper industry respectively. Contrary to succinic and maleic anhydride head groups[15] as well as dimer fatty acids[16] – commercially available as technical mixtures of isomers on the ton scale – ASA derived head groups have not yet been proposed for the synthesis of bola-amphiphiles to the best of our knowledge.

This article is divided in four parts. The first chapter describes the synthesis and molecular diversity of the polymeric bola-amphiphiles. The formation and characterization of their aqueous dispersions are given in the second chapter. The third section addresses the role of different ASA derived terminal side chains, which was studied in monomeric diester based bola-amphiphiles. Finally the systems studied are put into the context of shorter homologues that resemble Gemini surfactants as well as non-bola type amphiphilic polyester.

Experimental

Materials. Distilled dimer fatty acid **A2** [CAS 61788-89-4, 3,5 meq acid, PRIPOL 1012, Croda Ltd.], hydrogenated bisphenol-A [CAS 80-04-6, 7,92 meq hydroxyl, Aceto Corp., USA], 1,4-bis (hydroxymethyl)cyclohexane [CAS 105-08-8, 99%, Sigma-Aldrich], hydrogenated phthalic anhydride **A1** [CAS 85-42-7, 95%, Sigma-Aldrich] and dimethyl ethanolamine [CAS 108-01-0, > 98%, Sigma-Aldrich] were used as supplied. Succinic anhydride [CAS 108-30-5, 99%, DSM], maleic anhydride [CAS 108-31-6, 99%, Sigma-Aldrich] trimellitic anhydride [CAS 552-30-7, > 97%, Sigma-Aldrich], alkenyl succinic anhydride **2c** [CAS 26680-54-6, > 97%, Trigon], **2d** [CAS 19780-11-1, 95% Sigma-Aldrich], **2e** [CAS 25377-73-5, > 96%, Merck], **2f** [CAS 26544-38-7, > 98%, Trigon] and **2g** [mixture of CAS 28777-98-2 and CAS 32072-96-1, >93%, Trigon] were used as obtained. Butan-2-one [CAS 78-93-3, 99,5%] was dried over molecular sieve (4 Å) for 24 h before use. Deionized water was used throughout all experiments.

Synthesis. Polyester **1** (PES) was synthesized from an equimolar mixture of **A1** and **A2** together with hydrogenated bisphenol-A using a diol to diacid ratio of 2,26 under nitrogen and stirring at 190°C and distillation of water until an acid functionality below 0,15 meq of the reaction mixture was reached. Polyester PES-NB was obtained from addition-condensation reaction of 72,7g **1** (2,55 meq hydroxyl) with 8,35g trimellitic anhydride under nitrogen and stirring and water distillation at 160°C until an acid functionality of 0,62 meq was reached. For the bola-amphiphiles **3**, **4** and **5,** the polyester **1**, hydrogenated bisphenol-A and 1,4-bis (hydroxymethyl)cyclohexane respectively were reacted with sub-stoichiometric amounts of 0,9 equivalents cyclic anhydride **2** per hydroxyl at 95°C in 2-butanone under stirring and under dried nitrogen until 100% anhydride conversion according titrations under aqueous versus non-aqueous condition.

Dispersion. All polymeric amphiphiles **3** and PES-NB were neutralized using 0,95 equivalents dimethyl ethanolamine per acid at 80°C followed by addition of water and distillation of 2-butanone until a content < 0,5 weight-% was reached. Water was added to adjust the amphiphile concentration, expressed as w value for the ammonium salts, before the mixture was cooled to ambient temperature. For amphiphles **4** and **5** the same procedure was applied using a temperature of 60°C.

Characterization. Small-angle X-ray scattering (SAXS) was recorded on the ID02 - high brilliance beamline of ESRF, Grenoble, France using monochromatic radiation (λ = 0,1 nm), a source-sample distance of 55 m and sample-detector distances (max range 1 to 10 m) to cover a typical q-range of 0,3 to 4,3 nm^{-1} (0,03 to 6 nm^{-1} for **3a** and **3b**). Intensities were corrected for empty mica platelets that were used as sample holder.

^{2}H-NMR spectra were measured with an Agilent VNMRS 500 MHz spectrometer at a resonance frequency of 76,717 MHz, with a spectral width of 7700 Hz, 80 transients, a pulse width of 20 μs (π/2) and an acquisition time of 0,3 sec. Samples were pre-equilibrated for 10 min. The heating rate was 2,5 °C / min.

Polarization light microscopy (PLM) pictures were taken by an Olympus BX51 microscope equipped with an UM Plan FI-lens and a XC10 digital camera. A droplet of the sample, conditioned at room temperature was prepared between a glass slide and a cover slip. For temperature depending PLM a Leitz Orthoplan light microscope equipped with a Linkam temperature control unit with liquid nitrogen cooling unit LNP, TMS 94 was used.

Cryogenic atomic force microscopy (cryo-AFM) was recorded using a Bruker Dimension Icon equipped with a FastScan ScanAsyst scanner and a Veeco DI TA controller. Samples were prepared using a Reichert Ultracut S sectioning system equiped with FCS cryo extension. A droplet of the sample was deposited on a metal attachment and microtomed at -80°C after a resting period of 15 min under ambient conditions. The frozen, truncated sample was transferred to the precooled stage (-20°C). AFM recording started after complete sublimation of formed ice crystals (approx. 15 min) using a frequency of 15 Hz.

Cryogenic transmission electron microscopy (cryo-TEM) was performed on a FEI Tecnai G^2 electron microscope using 200 kV as accelerating voltage. Ultrathin sections (70 nm) of the sample were cut at -80°C using a Leica UC6 ultra-microtome equipped with a Leica EM FCS cryo chamber and a diamond knife.

Rheological characterization of the bola-amphiphiles **4** was performed on an Anton Paar MCR302 CP25/1° rheometer for amplitude and frequency sweeps at 23°C using a cone plate distance of 0,05 mm at a constant frequency of 1 Hz and a constant amplitude of 0,1 mrad covering $8{,}8*10^{-3}$ to 1000 mrad and 1 and 100 Hz respectively. Temperature dependant measurements were performed on an Anton Paar MCR501 CP50/1° rheometer using a cone plate distance of 0,099 mm at a constant frequency of 1 Hz and an amplitude of 5,8 mrad and applying a constant heating rate of 1K/min covering 20 – 90°C.

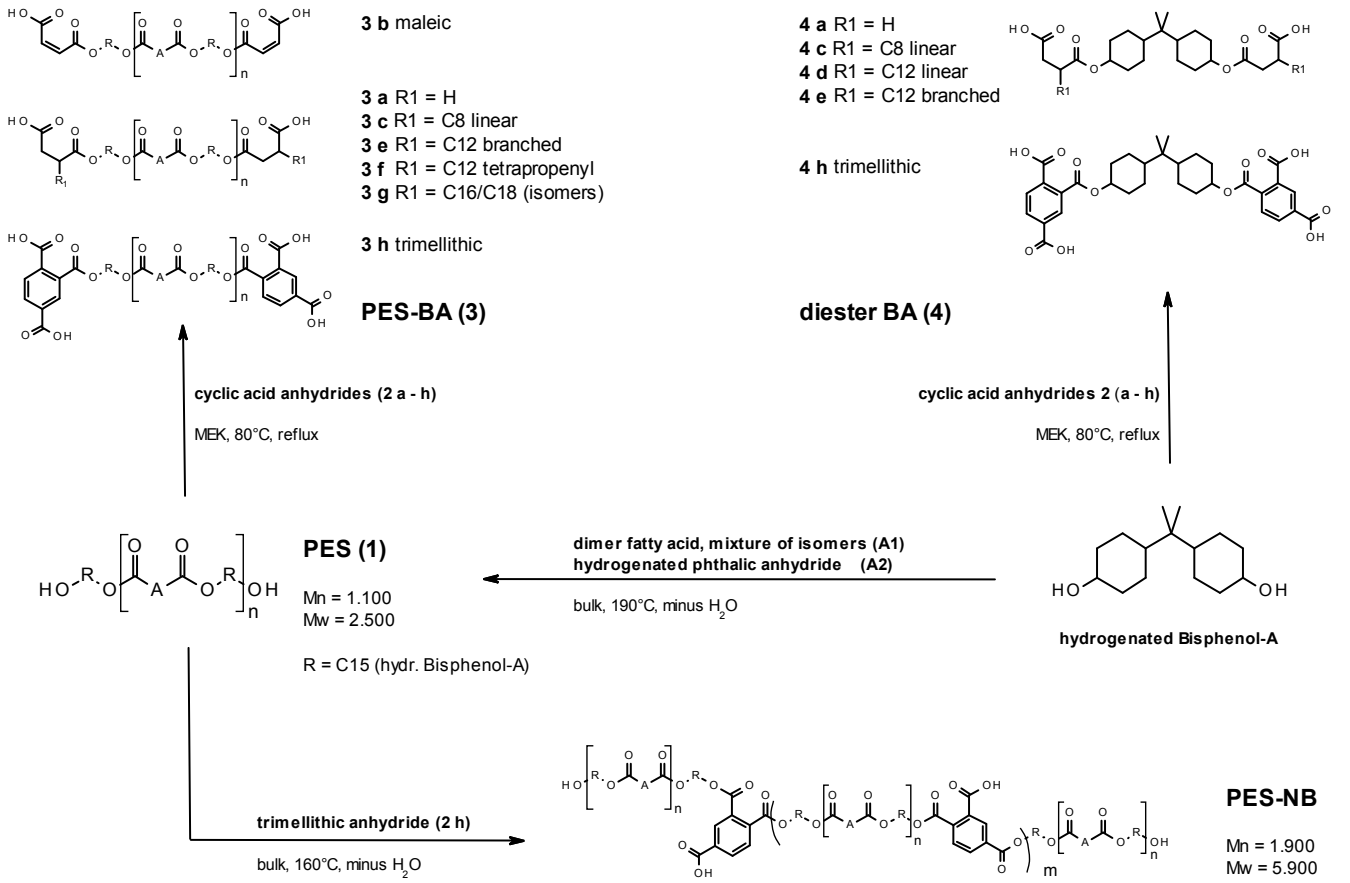

Fig. 1 Survey of synthesized polymeric bola-amphiphiles (**3**) based on the α,ω-polyesterdiol PES (**1**), hydrogenated bisphenol-A derived diester bola-amphiphiles (**4**) and the non-bola-amphiphile PES-NB obtained from (**1**) in an addition-polycondensation process. Increment '**A**' in **(1)** symbolizes a mix of A1 and A2 (see experimental part). For structures **(3)** and **(4)** with R1 ≠ H and trimellithic head groups asymmetric molecules represent isomerism with R1 in α- or β-position and the pristine CO_2H group in meta or para position respectively (see text). Replacing HBA by 1,4-bis(hydroxymethyl)cyclohexane (CHDM) corresponding diester with **2a**, **2c** and **2e** have been synthesized to yield **5a**, **5c** and **5e** respectively, that are omitted for clarity.

Rheological characterization of PES-NB was performed using a Haake MARS system (Thermo Scientific) with a 2° titanium cone and a glass plate (gap width 70 µm), temperature-controlled by a Haake thermostat. For temperature dependent measurements appropriate steps were defined. Only data after stabilization ($\Delta T < 1K$) that fulfill the harmonic approximation were used. These were taken at 10 Pa and 100 Pa and a frequency of 1 Hz over a period of at least 3 min on each stress level. Due to high viscosity of PES-NB dispersions the gap might not always be filled completely in its outer part. Therefore absolute values of G′ and G″ may be offset and should be compared directly only in individual measurement runs.

Simulated systems contained various isomers of **4c**, counter ions and water yielding a total N=16000 atoms their proportions adjusted to concentrations of the organic phase (**4c** plus counter ions) in the range of $0,3 \leq w \leq 0,6$. All molecular dynamics simulations were carried using LAMMPS[i] (1) within an NPT ensemble, i.e. at constant pressure and temperature (p = 1 atm, T = 298.15 K) and an integration time step of one femtosecond. Interatomic potentials were described by the COMPASS[ii] force field and VMD[iii] was used for analysis and visualization.

[i] *J. Comp. Phys., 1995,* ***117****, 1; Sandia National Laboratories, Large-scale Atomic/Molecular Massively Parallel Simulator (LAMMPS 1995-2011) (http://lammps.sandia.gov).*

[ii] *J. Phys. Chem. B, 1998,* ***102****, 7338.*

[iii] *J. Mol. Graphics, 1996,* ***14****, 33.*

Results and discussion

Amphiphilic polyester: synthesis and structure

All polymers are based on a hydrophobic α,ω-polyesterdiol (PES) which is obtained from the esterification between hydrogenated bisphenol-A (HBA) and a 1:1 molar mixture of hydrogenated phthalic anhydride (HPA) and dimer fatty acid (DFA). Nucleophilic addition of the terminal hydroxyl groups on a cyclic anhydride (SA, MA, ASA, TMA) converts PES into telechelic carboxylic acid terminated polyester, namely a polymeric bola-amphiphile PES-BA (fig. 1). For the non-bola polyester PES-NB ring opening of TMA is followed by polycondensation which formally yields chain extended PES with residual mid chain carboxylic acid groups. Molecular weight distributions from SEC (fig. 2a) show that PES **1** consist

of numerous different species reflecting both the mass and size difference between the C8 and C36 based synthons A1 and A2 respectively as well as a different reactivity between HPA (anhydride) and DFA (free acid) towards the hydroxyls of HBA. The latter was chosen because of its combined hydrophobicity, stiffness and hydrolytic stability of the formed ester bond. However this goes along with a low reactivity in the esterification and anhydride ring opening which entails prolonged synthesis compared to primary alcohol esterification. For compensation we used an unusual high diol to diacid ratio (2,26) that in theory does not allow for polymer formation. Without further analytical evidence relating to the chemical nature of the different SEC fractions it is evident that PES must consist of oligomers besides diester and excessive HBA. This is corroborated by the size exclusion chromatogram of **4c** which is shown for comparison in figure 2b. Thus non-equilibrium reflects kinetically favoured esterification between HPA (ring opening) and "trans" isomers of HBA (least steric hindrance). It has to be noted that the HBA quality we used consists of three isomers with respect to hydroxyl ring position. Related to bis-equatorial configured isopropylidene moieties equatorial and axial positioned hydroxyl groups account for a dominating trans,trans isomer (w = 0,5), a cis-trans isomer and a minor portion (w = 0,1) of a cis,cis isomer (see ESI). Assuming fastest reaction of trans,trans HBA with HPA due to least steric hindrance and ring opening and a higher reactivity of DFA compared to that of the HPA-HBA addition product (steric hindrance in the latter), the most probable intermediate would be HPA-HBA-DFA which in turn would preferentially consume trans,trans-HBA followed by trans,cis-HBA. Thus residual HBA should consist of enriched cis,trans- and cis,cis-HBA. These most probable species are highlighted in a list of all combinatory conceivable bola-amphiphiles of exemplary **3c** indicating molecular weights and lengths in all-trans configuration (Table S1). Molecular diversity in PES additionally stems from non-uniformity of DFA that comprises numerous isomers regarding the 'connecting' moieties, best described as products of an ene-reaction and a cycloaddition.[16] Thus linear and cyclic increments with varying proportions of saturated aliphatic, unsaturated and aromatic bonds depending on process parameter and optional post hydrogenation are common. The quality we used comprises minor amounts of mono- and tri-functional species (cf. experimental part). Regarding the SEC curves (fig. 2) we emphasize that no absolute molecular weights can be deduced due to PMMA standards. However comparing distributions of PES with different PES-BA (**3a**, **3c**) and diester (**4c**) it is obvious that the prominent peaks fall into the range of theoretically deduced molecular weights (vide supra, cf. table S1). Noteworthy the shape of the curves found for **3a** and **3c** indicates an impact of the head groups on the hydrodynamic radius. As expected for PES-NB, the mean molecular weight and the dispersity (Mw/Mn) are considerably higher (fig. 2c).

Regarding the amphiphiles of series **3** and **4** molecular complexity increases after ASA and TMA ring-opening which yields ester groups bearing an alkenyl chain in α- or β-position or the pristine carboxylic acid group in para or meta position respectively (cf. Fig. 1). Finally for a given ASA type branching and cis / trans isomerism of the aliphatic group adds to molecular plurality.

Therefore we studied the impact of the length (C8, C12, C16/C18) and the structure (linear, branched) of the alkenyl side group. Numerous different ASA qualities are commercially available. Typically synthesized from maleic anhydride and α-olefins in an ene-reaction it is known that mixtures of branched products are obtained under process conditions where the olefinic double bond is prone to migrate chain inwards.[17] Thus at least three different materials are labelled "dodecenyl-SA": a rather pure chemical comprising two (cis, trans) linear C12 chains (**2d**), a mixture of isomers with respect to branched C12 chains stemming from an undefined precursor or an in-situ scrambled linear α-olefin (**2e**) and finally an isomer mixture based on tetrapropenyl (**2f**). While the short C8 ASA (**2c**) consists of two linear species (cis, trans) the C16/C18 ASA (**2g**) shows two sets of numerous isomers for the two different chain length. We compared these ASA terminated PES-BA with those bearing succinic (**2a**), maleic (**2b**) half ester as well as the addition product from TMA (**2h**).

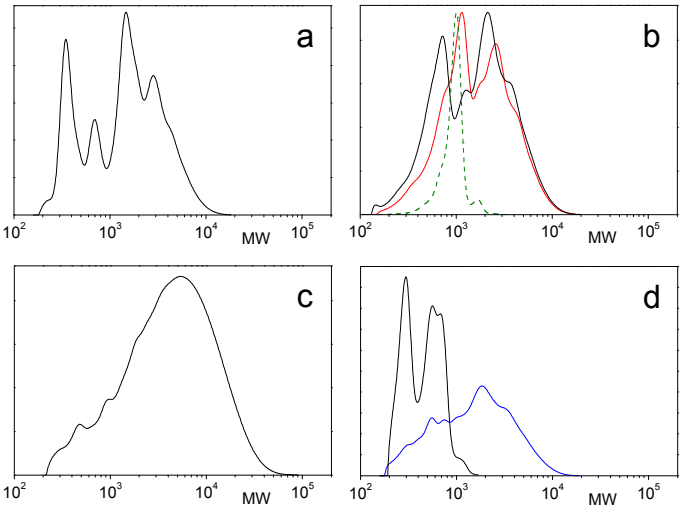

Fig. 2 Molecular weight distributions of (a) PES (**1**), (b) polymeric bola-amphiphiles **3a**,(black) and **3c** (red) and diester bola-amphiphile **4c** (green, dashed), (c) non-bolaform PES-NB, (d) separated lamellar phase (black) and isotropic phase (blue) of polymeric BA **3a** (w = 0,54).

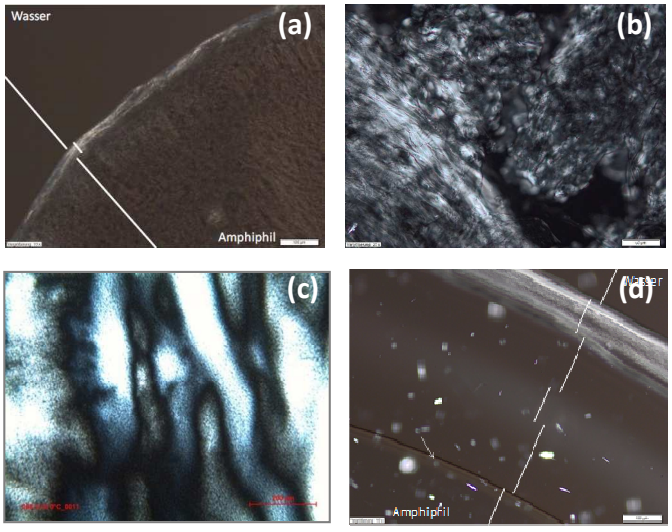

Fig. 3 (a) Contact preparation of **3a** showing a myeline like interphase diagonally demarcating water (to the left) and the amphiphile (scale bar 100 µm), (b) PLM picture of phase separated lamellar phase of **3a** (w = 0,54) (scale bar 50 µm), (c) PLM picture of **3c** at 0°C (w = 0,33) (scale bar 200 µm), (d) contact preparation between **3f** (w = 0,82) showing batonnets and water (upper left) (scale bar 100 µm).

Mesophases from PES-BA

For dispersion into water the amphiphiles acidic groups were transformed into the ammonium salt of dimethyl ethanolamine.The PES-BA (**3a–3h**) have been dispersed in water covering a concentration range of 0,3 < w < 0,8 (w = weight fraction of PES-BA). For this purpose samples were taken from a dilution process of a concentrated stock solution (w ~ 0,8) at 80°C. However with succinic and maleic terminated PES-BA (**3a**, **3b)** homogeneous mixtures could not be obtained for mixtures below w = 0,5 which was confirmed by contact preparations for polarized light microscopy (PLM) under ambient conditions. These showed a quick formation of a myelin like phase near the borderline that did not change within hours (fig. 3a). We interpret these findings with the formation of extended lamellae. These impede or significantly retard further dilution but can swell. Indeed SAXS peaks in the ultra-small angle region for both systems correspond to 100 – 200 nm large objects (shown for **3a**, fig. S2). Such a huge spacing of swollen BA based lamellae is not unusual[18] and has also been reported for dilute ASA-water systems.[19] Upon standing over several months **3a** (w = 0,54) macroscopically phase separates into an isotropic phase (no birefringence, no peaks in SAXS) beneath a lamellar phase as indicated by three harmonic peaks with a corresponding repeat distance of 7,9 nm (PLM: fig. 3b, SAXS: fig. 4a). These phases consist of distinct different PES-BA species of **3a**. While a low molecular weight fraction build the lamellar phase, the isotropic contains polymeric amphiphiles (fig. 2-d).

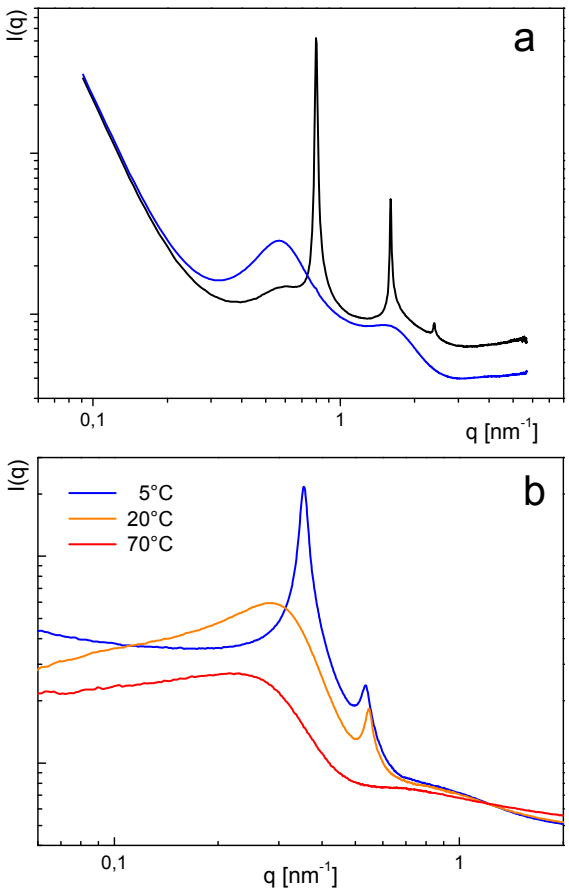

Fig. 4 SAXS curves obtained on (a) phase separated (**3a**) w = 0,54 into a lamellar (black, d = 7,88 nm) and an isotropic phase (blue), (b) peaks of (**3c**) w = 0,33 at 5°C, 20°C and 70°C.

For ASA terminated PES macroscopic homogeneous and storage stable dispersions could be obtained down to w ~ 0,3. Apart from peculiarities reflecting an impact of the nature of the alkenyl side group all PES-BA **3c** – **3g** show ordering somewhere within the parameter space defined by temperature (0° - 80°C) and composition (0,3 < w ≤ 0,6) according to SAXS reflections (listed, table S2) and birefringence textures. Except for **3g** these peaks shift to lower q values with decreasing concentration indicating larger distances or objects. Besides these reflections humps appear which will be discussed below.

Thus PES-BA **3c** (C8 chains) at w = 0,33 shows increased ordering upon cooling from 20°C to 5°C where the hump transforms into a sharp peak (fig. 4b) while the Schlieren-like birefringence, typical for nematic ordering, becomes more intense (fig. 3c). Both vanish at higher temperatures, shown for SAXS at 70°C. A similar, less pronounced temperature dependence was found with PES-BA **3f** (tetrapropenyl C12) at w = 0,49 where the hump only appears upon cooling. With increasing concentration **3f** forms ***batonnets*** as was shown with PLM in a contact preparation (fig. 3d).

The isomeric **3e** (branched C12 chains) does not show any birefringence between 0,34 ≤ w ≤ 0,47 below 50°C. This might be due to homogeneous alignment as SAXS displays both types of reflections. Above 50°C birefringence without texture of an ordered isotropic, e.g. bicontinuous, phase appears. At lower concentration (w = 0,31, not shown) this was found within huge isolated domains of a non-birefringent liquid.

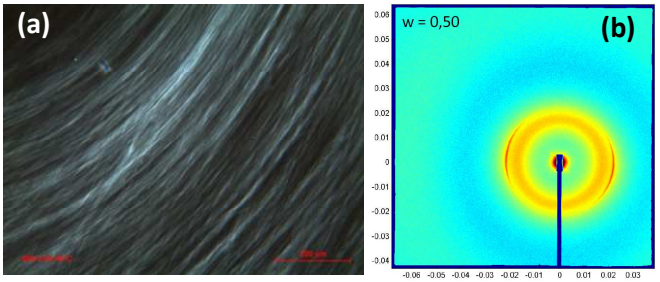

Fig. 5 (a) Birefringence of **3g** (w = 0,5) at 40°C (scale bar 200 µm), (b) 2D SAXS pattern of the same phase at 20°C, showing an oriented mesophase with respect to the peak positions at q = 0,46 nm^{-1}.

Increasing both the length and the non-uniformity of the aliphatic chains in **3g** (branched C16 and C18 chains) leads to aqueous compositions (w = 0,5 – 0,6) that show anisotropy in SAXS (fig 5b). The birefringence texture of shear banded oily streaks persists up to 50°C and is evocative of a lamellar phase (fig. 5a). However the correlation length is rather limited regarding missing harmonics.

In conjunction with the morphological variety of mesophases formed by bola-amphiphiles in binary systems with water over vast concentration and temperature ranges[8] the clarification of the self-assembly of PES-BA **3a** to **3g** during the manufacturing procedure remains a matter of further studies, e.g. in-situ SAXS measurements. However with regard to reported bi-layered membrane formation in concentrated C16-ASA solution[19] and the shift from vesicle to disk formation in bola-amphiphile water systems with increasing temperature from 20°C to 60°C[12] we assume that the PES-BA tend to adopt layered assemblies in the course of the dilution process. This is corroborated by our findings on the dilution of succinic and maleic ester bearing PES-BA **3a** and **3b** resp. (vide supra), distinct peaks (1st and 2nd harmonic) in

concentrated phases of TMA terminated PES-BA **3h** (table S2, n.b.: double ionic strength) as well as indications for lamellae formed by ASA terminated PES-BA **3g**. Contrary to the succinic (and maleic) terminated counterparts, the latter can be further diluted and does not phase separate. This suggests either the presence of less extended or porous lamellae and (or) intermolecular stabilization via hydrophobic attraction of the terminal hydrophobic side chains.

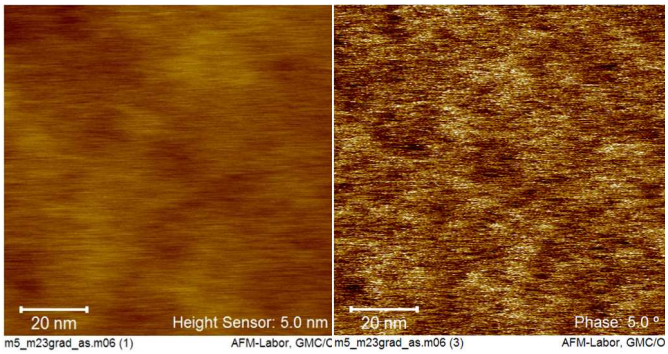

Fig. 6 cryo-AFM images (topography left, phase contrast right) of **3c** (w = 0,4) frozen at 0°C reveal aligned domains with dimensions and spacings in the order of 10 to 20 nm respectively, resembling nematic order.

However in the case of ASA head groups that bear shorter (linear or branched) chains stabilization seems to favor finite anisotropic objects like rods, disks or ribbons that tend to nematic ordering (cf. **3c**, **3f**). Indeed cryo-AFM imaging of surfaces from PES-BA **3c** (w = 0,4) (fig. 6) and **3f** (w = 0,49) (fig. S1) suggests preferentially aligned anisotropic objects of dimensions and spacing that are roughly corresponding to observed humps and peaks in SAXS (appr. 10 – 20 nm).

These humps might reflect a 'correlation hole effect' rather than an ordering phenomenon: only by using a high flux X-ray source Cortese et.al. observed broad reflections in bolamaphile dispersions and attributed them to the distance between electron richer heads attached to the aliphatic spacer.[20] However with regard to the esterification process of PES (vide supra) this interpretation would imply unlikely high proportions of high molecular weight species, e.g. **2c** capped HPA:DFA:HBA = 3:3:7 (18,3 nm, table S1), that could cause humps around 20 nm. As their positions shift to lower q values with decreasing w values (table S2) we assume that they reflect disordered dispersion states of discrete objects consisting of assembled bola-amphiphiles. This is in line with the hump to peak transition in the scattering curves of **3c** (w = 0,33) during cooling (fig. 4b).

Such objects may be formed by co-assembly of polymeric and diester based bola-amphiphiles (cf. composition of PES) while anisotropy arises from their different molecular dimensions of ~ 5 to 10 nm versus ~2 nm respectively (cf. table S1 and table S2, peak positions). There is a pronounced shift of the peaks around 7 nm to values around 10 nm with decreasing concentration for all ASA bearing systems. This shift is much less for higher w values of **3h**. We interpret this by a variable degree of chain elongation of longer, flexible amphiphiles, especially DFA comprising ones, in response to favorable charge separation as a function of the number of ionic groups (higher for **3h**) and the degree of dissociation which should increase upon dilution. For the succinic ester and ASA based systems accommodation of oligomers with intermediate molecular weight and dimensions has to be considered and discussed in the context of lower degrees of carboxylic acid neutralization. Indeed considerable amounts of amine evaporated in the course of sample preparation (table S2). Consequently, as a function of water content, varying amounts of not neutralized acid groups of shorter bola-amphiphiles could be embedded within the hydrophobic core of the assemblies (fig. 7). Such an accommodation seems reasonable in the light of similar findings reported for glycerol terminated asymmetric bola-amphiphiles.[8, 21]

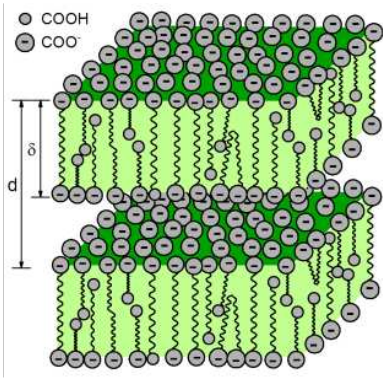

Fig. 7 Assembly model of polymeric bola-amphiphiles of different length, symmetry (carboxylic acid, carboxylate) and conformation (stretched, bended). Dimensions are not to scale.

The different behavior of succinic and alkenyl succinic bearing amphiphiles reveals a twofold role of hydrophobic side chains neighboring the polar head group:

(i) stabilization of assemblies of different species and
(ii) packing frustration that impedes lamellae formation.

To summarize the results we have shown that ordered mesophases can be obtained from an ill-defined system of bola-amphiphiles comprising monomeric and polymeric species and that the presence and the nature of terminal hydrophobic side groups have a distinct impact on the assembly and thus the degree of order of the obtained dispersions. In the following chapter ordering phenomena of ASA based HBA are described in more detail.

Mesophases from monomeric diester bola-amphiphiles

Hydrogenated bisphenol-A alone – despite being rather bulky and hydrophobic – apparently fails to provide a suitable hydrophobic spacer for the diester **4a** (succinic) and **4h** (trimellitic). The corresponding ammonium salts do not show any birefringence in contact preparations and in bulk **4h** quickly dissolves as bola electrolyte (not shown). In order to shed light on the assembly of ASA terminated PES-BA, reference compounds **4c** (linear C8), **4d** (linear C12) and **4e** (branched C12) have been prepared and their aqueous mesophases studied. Apart from their uniform molecular weights these compounds, like their polymeric counterparts, consist of molecular mixtures regarding isomerism of the diol, the alkenyl chain and its position relative to the succinic ester group (vide infra).

Although heating would be unnecessary with regard to low viscosities compared to the concentrated PES-BA, the neutralized diester were diluted with water at temperatures above 60°C. Thus homogeneous, transparent and storage stable

dispersions were obtained either in the form of gels or viscous fluids in the concentration range 0,3 ≤ w ≤ 0,7. In contrast, dilution of **4e** at room temperature yields heterogeneous mixtures of coarsely dispersed white waxy solid, indicating metastable regions in the phase diagram of this system.

Structural analysis of the aqueous phases of **4c**, **4d** and **4e** reveals a common feature in SAXS: two more or less pronounced peaks at positions in line with lamellae of decreasing spacing with increasing bola-amphiphile contents as shown for **4c** (fig. 8). At lowest concentration the main reflex is rather broad and the second peak barely visible as a step while at w = 0,4 faint peaks of inverted intensities are found (besides a weak 3rd harmonic). For higher concentrations peak intensities raise. Similar sets of peaks are found for the mesophases of **4d** and **4e** (fig. S3, table S4). However for the linear C12 chains these are only present at higher bola-amphiphile contents (w ≥ 0,6). Compared to the corresponding C8 based phase the repeat distance increases about 0,63 nm (w = 0,7), which nearly matches twice the length of an all-trans C4 increment (0,312 nm). At lower concentrations broad humps indicate poor ordering. Intriguingly the branched C12 groups impede ordering at the highest concentration while the abnormal peak intensities described above for **4c** (w = 0,4) are shifted to a concentration of w = 0,5. Compared to the other amphiphiles at w = 0,7 the differences of the peak (or hump) positions translate into roughly half the distance found for the comparison between **4c** and **4d**, specifically 0,34 nm larger than in **4c** and 0,29 nm smaller than in **4d** (table S4). This would be in line with a less extensive space filling of the branched chains in **4e**. Although plausible with regard to molecular extensions the difference between repeat distances in **4c** and **4d** at high w values can hardly be explained by a typical bola-amphiphile assembly. Such lamellar stacking between aligned hydrophobic spacer and water with the polar heads forming the interface implies that the alkenyl chains should oriented inbound rather than into the water phase. However a bilayer type assembly of molecules with their two hydrophobic side chains being oriented asymmetric and two elongated ones forming the hydrophobic core of a lamella that comprises water inclusions (pores) could explain the findings.

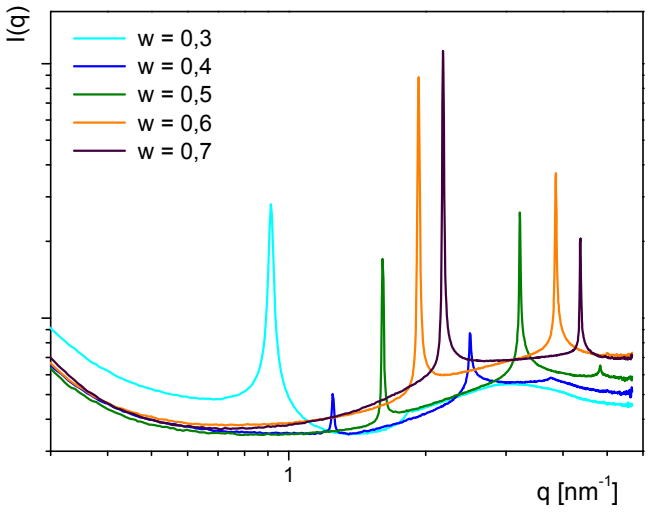

Fig. 8 SAXS curves from phases of **4c** at 0,3 < w > 0,7 and 20°C. Peaks shift to higher q values with increasing w.

All phases at w = 0,3 except for **4c** (fig. 9a) and those at higher w values which only show humps in SAXS do not display any birefringence. Remarkably those which cause faint and unusual SAXS peak ratios exhibit distinct shear dependent birefringence with oily streaks transforming into a marble texture (**4c** w = 0,4 fig. 9b and 9c) or into the dominant Maltese crosses (**4e** w = 0,5 fig. 9d) respectively. Such behaviour is evocative of lamellar polymorphism observed in several bilayered assemblies of two- and multi-component aqueous detergent mixtures. Thus the evolving texture of **4e** (w = 0,5)[22] could be indicative for a transition of a lamellar phase (L_a) into a multi-lamellar vesicle (L_{a1}) phase.[23] Indeed a cryo-SEM image of this mesophase reveals a lamellar morphology comprising domains with a distinct curvature (fig. S5). For the texture change of **4c** (w = 0,4) polymorphism between an isotropic sponge (L_3) and a lamellar (L_α) or mesh phase respectively is reasonable.[24] The former is known to readily align under external force into the latter, both sharing scale invariance[25] and form in concentrated regimes and persist into dilute regions.[26]

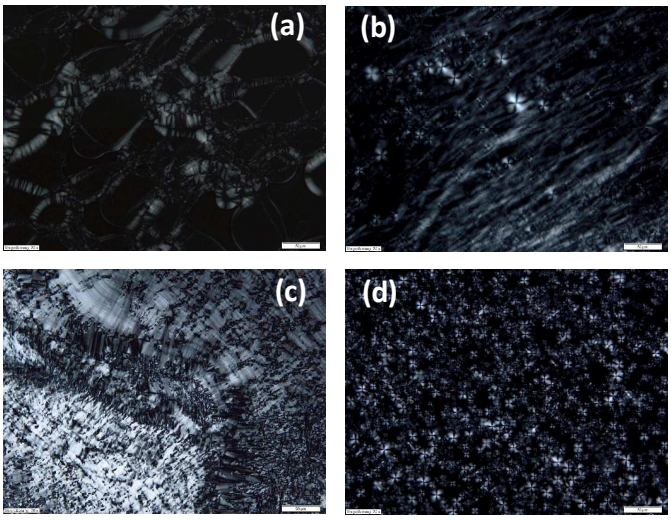

Fig. 9 PLM pictures of (a) **4c** w = 0,3, (b) **4c** w = 0,4), (c) same as in (b) after shearing the cover slip, (d) **4e** w = 0,5. All scale bars 50 µm.

These observations are corroborated by ^{2}H-NMR experiments on corresponding samples, dissolved in D_2O on an equimolar basis with regard to the H_2O based counterparts. The extent of the ^{2}H quadrupole splitting depends on the degree of anisotropy at the amphiphile water interface and thus indicates the symmetry of the mesophase as well as the samples heterogeneity in the case of coexisting mesophases of different space groups.[27] Curves of the mesophases of **4c** (fig. 10) show biphasic samples for w = 0,3 (main portion isotropic, compare with birefringence, fig. 9a) and w = 0,4 (a set of peaks and shoulders respectively). At higher concentrations the anisotropy of the interface and thus the splitting increase to values typical for lamellar interfaces (peak separation ~ 1.700 Hz).[28] However the smooth "filling" between the peaks indicates the presence of more isotropic parts in these interfaces. Similar behaviour is found for **4d** and **4e** (fig. S4). Their less ordered phases (humps in SAXS curves, vide supra) do not show quadrupole splittings while for the ordered concentrated phases of **4d** the splitting equals that of **4c**. For the branched C12 bearing bola-

amphiphile **4e** maximum splitting is much less (644 Hz) compared to that of both other systems.

While the structural analysis of the ordered phases reveals isotropic features of a lamellar morphology rheological properties of these phases accentuate the isotropic aspect. Indeed amplitude sweeps reveal a distinct gel character of **4c** over the whole concentration range with G' exceeding G'' by factors of 6 to 15 and yield points between 5 and 45 Pa.[†1] This could best be described with a percolating, force transducing, bicontinuous morphology. The ordered phases of **4d** ($w \geq 0,6$) and of **4e** ($w < 0,6$) show a similar behaviour while the less ordered phases (humps in SAXS) of both **4d** ($w < 0,6$) and **4e** ($w > 0,6$) are viscous fluids. This is exemplary shown for the phases at w = 0,5 (fig. 11) and leaves **4e** at w = 0,6 as an exceptional dispersion where order and viscous behaviour coincide.

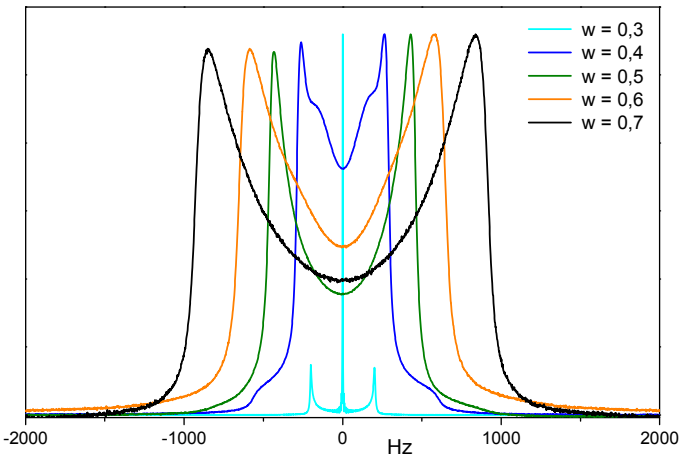

Fig. 10 ^{2}H-NMR of **4c** in D_2O showing deuterium quadrupole splittings increasing with concentration (w-values are rounded, see experimental part). At w = 0,3 (compare OPM picture, fig. 9a) and w = 0,4 sample are biphasic.

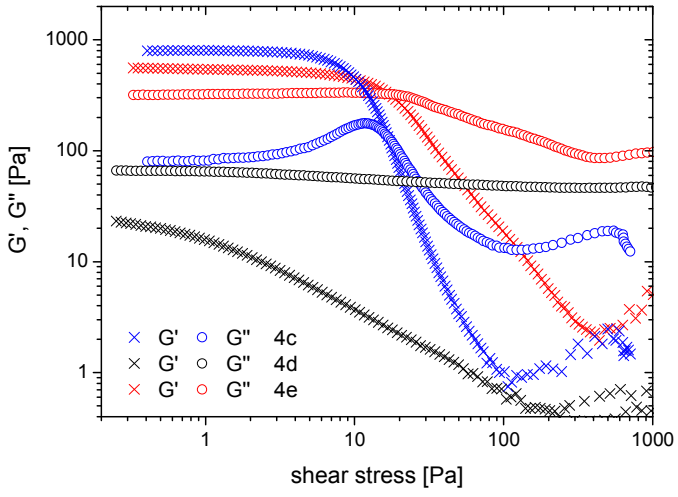

Fig. 11 Amplitude sweeps performed at 20°C and 1Hz on the mesophases comprising of distinct hydrogel **4c** (blue), viscous fluid **4d** (black) and hydrogel **4e** (red) at w = 0,5. Storage modulus G' (crosses), loss modulus G'' (circles).

For all ordered dispersions of **4e** ($0,3 < w < 0,6$) elasticity and viscosity considerably decline upon heating in the range of 35 – 60 °C, with higher concentrated phases becoming fluid more quickly (fig. S6a). This is accompanied by a loss of the anisotropic structure, revealed by quadrupole splitting (fig. S6b). Noteworthy inverse behaviour takes place with **4d** at w = 0,5. Isotropic and viscous at room temperature, this system forms a coexisting anisotropic part upon heating (fig. S7b). This transforms the viscous liquid into an elastic dispersion at 50°C (fig. S7a). All dispersions of **4c** and the ordered phases of **4d** retain moduli at least up to 80°C or 90°C (**4c** w = 0,5, **4d** $w \geq 0,6$) respectively (fig. S8a, fig. S7a). For **4d** (w = 0,7) an isotropic fraction is formed around the yield point which dominates in the fluid region (fig. S7b) while only slight changes in the quadrupole splitting of **4c** based dispersions were observed until 80°C like the merger of the coexisting curvatures at w = 0,4 (cf. fig. 10) into one anisotropic phase around 60°C (fig. S8b).

To summarize the experimental results we have shown that HBA based bola-amphiphiles with C8 – C12 ASA head groups self-assemble in the water phase into anisotropic structures resembling mesh and coexistent bicontinuous phases. With regard to the terminal hydrophobic side group the linear C12 system fails to maintain ordered assemblies with increasing dilution whereas non-uniform, bulky groups of the branched C12 system impede ordering at high concentration and the formation of temperature stable structures in dilution. On the contrary linear C8 groups allow for ordered structures over the entire range of covered concentrations and temperatures.

With regard to the polymorphism we suggest that molecular diversity of the diester bola-amphiphile most probably impedes the formation of different well-defined, e.g. lamellar assemblies. We calculated a possible composition of **4c** (the same would apply to **4d**) on the basis of analytical results regarding isomerism of educts and reaction products. As outlined in the supplementary information HBA consists of five species. Apart from two minor unassigned monools the diol (w = 0,97) comprises a trans,trans (w = 0,50), a cis,trans (w = 0,42) and a cis,cis (w = 0,08) isomer. ASA **2c** consists of trans- and cis-configured double bonds in the unsaturated chain in a 4:1 ratio. Anhydride addition yields two different succinic ester groups with alkenyl chains either in α- or β-position (α/β = 0,61). Lacking further information concerning symmetry with respect to isomeric head groups in **4c**(**d**) we assume independent probabilities and ignore the monool fraction. Thus 35 different species in proportions between 21,73 and 0,97 mol-% (table S3) are obtained. On this basis it is reasonable that bola-amphiphiles of different shape (e.g. cis,cis vs. trans,trans) and varying distance between the hydrophobic chains (e.g. α,α- vs. β,β) can be allocated to sites of different curvature in order to minimize packing frustration. Thus molecular diversity induces polymorphism of a few rather similar structures over a broad concentration range, contrary to molecular uniform systems that usually display morphological plurality with varying water content.[29] Indeed molecular simulations of **4c** in water in the range of $0,3 \leq w \leq 0,6$ yield anisotropic morphologies like biased bicontinuous phases (shown for w = 0,3, fig. 12) and porous lamellae. It is noteworthy that although slight changes in isomer compositions can generate qualitative changes in morphology, all of them resemble anisotropic meshes or bicontinuous phases. These results confirm the experimental findings and support our interpretation.

Thermal stability as well as order at very high concentration decreases in the case of branched side groups while longer

linear chains impede ordering at lower concentrations. The former is intuitively understood regarding the bulkiness of the hydrophobic moieties. For the longer chains most probably intermolecular hydrophobic attractions between just a fraction of differently shaped isomers induce rupture of the percolating assembly as it is evidenced by the fluid nature of the more dilute dispersions.

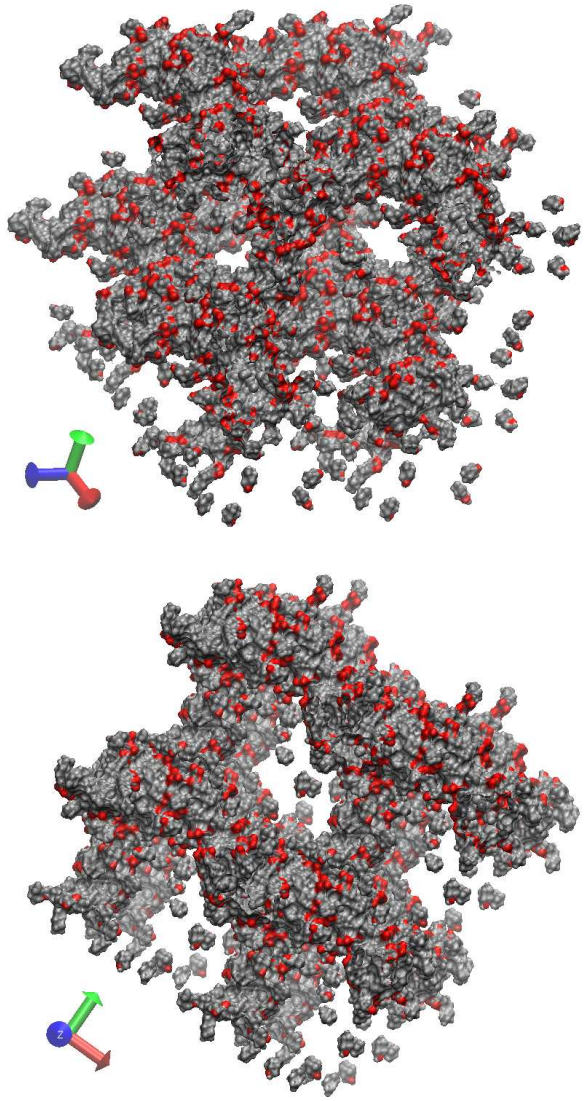

Fig. 12 Simulated bicontinuous morphology of **4c** in water (w = 0,3) after 100 ns at 20°C. Box size 16.000 atoms comprising 34 molecules of **4c**, taking into account the 15 most prevalent isomers (see text and table S3). Only the molecules of **4c** and the ammonium ions are shown (red = oxygen atoms) while the box is periodically repeated once in each direction (x, y, z) for clarity.

Bola-amphiphiles, bola-electrolytes and non-bola-amphiphiles

As mentioned in the preceding chapter compounds **4a** and **4h** do not form ordered assemblies in water[†2] as do the ASA based analogues. With respect to the latter we were interested in the question at which point with respect to the spacer length the ordering would be changed or impeded: where does the bola-amphiphile would transform into a Gemini surfactant or a bola-electrolyte respectively? We synthesized the diester from 1,4-bis(hydroxymethyl)cyclohexane (cis : trans = 0,43) with **2a**, **2c** and **2e** respectively in order to maintain the bulkiness and rigidity of HBA. However all dispersions of the neutralized diacids **5a**, **5c** and **5e** are transparent low viscous fluids that do not display any birefringence in OPM, contrary to the neat hydrolyzed and neutralized ASA who form well-defined mesophases in water which is shown for **2c** (fig. S9). Thus a shorter yet rigid spacer forces ASA based diester to dissolve as bola-electrolytes.

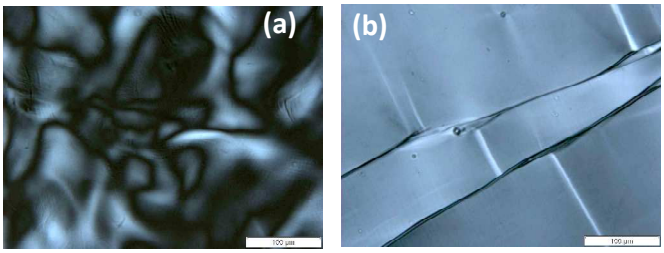

Fig. 13 PLM pictures of PES-NB in water (w = 0,35) (a) freshly prepared and (b) after 7d at ambient temperature.

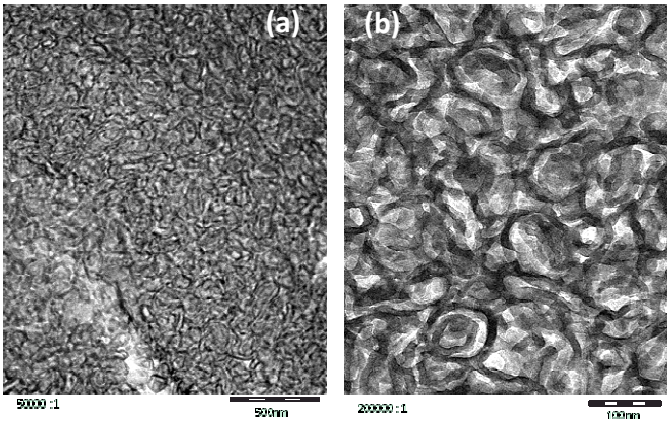

Fig. 14 Cryo-TEM images of an aged dispersion of PES-NB in water (w = 0,35) showing a truncated bicontinuous morphology (a) cross sectioned (scale bar 500 nm), (b) in projection (scale bar 100 nm).

In the preceding section the pronounced tendency of **4c** to form hydrogels of distinct temperature stability was shown, while PES-BA **3c** assembles into nanosized, nematic aligned objects. We expected a pronounced gel character for dispersions of higher molecular weight polyester that comprise angular chains or a branched architecture like PES-NB, a chain extended PES via TMA (fig. 1). The hydroxyl terminated polyester bears mid chain carboxylic acids. Dilution of the molten neutralized PES at 80°C yields homogeneous, translucent hydrogels in the concentration range $0,7 \geq w \geq 0,3$. With w = 0,35 a freshly prepared dispersion displays Schlieren texture of a nematic ordering which changes into featureless birefringence[†3] within few days (fig. 13). Cryo-TEM images, taken after several weeks, reveal worm like patterns of truncated bicontinuous phases (fig. 14). After 26 months at ambient conditions the gel still manifests its undulated surface (fig. S10) and tangibly oscillates in response to manual

knocking against the container. The distinct time dependency of the ordering that produces an elastic solid with a pronounced yield point prompted us to study the rheological development of the dispersion in the temperature range of 10 to 60°C. Heating causes an increase of the loss modulus (G'') until 30°C followed by a decrease of both moduli until, at 60°C, G'' dominates the storage modulus (G'). Comparing a freshly prepared with an aged sample the gel fluid transition starts on much higher viscosity level in the latter (not shown). Upon cooling of the heated sample the material follows simple Arrhenius behavior down to 30°C. Below that temperature G' increases further while G'' decreases, ending with an elastic solid at 10°C (fig. S11). The pronounced inertia of PES-NB is reflected by the slow development of the viscoelastic components over time at higher temperatures (fig. 15).

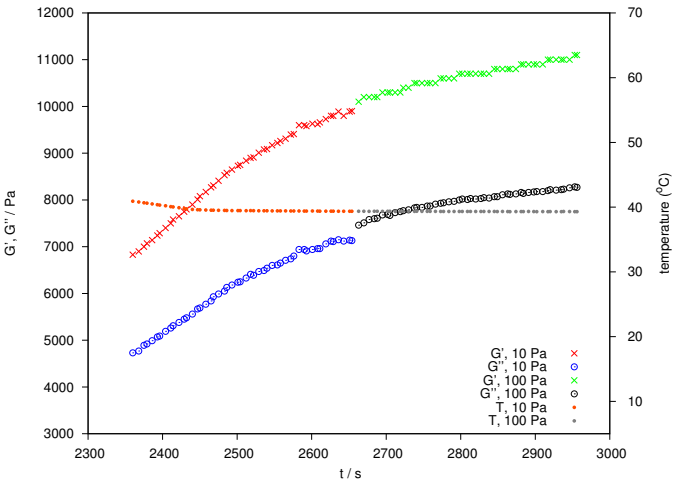

Fig. 15 Oscillating shear rheology on PES-NB in water (w = 0,35) at 40°C taken during the cooling phase of a preheated (60°C max.) sample. The evolution of loss (G'', circles) and storage (G', crosses) modulus in the time domain was followed at two different shear stresses (10Pa, blue and red and 100Pa, green and black).

Conclusions

The present study describes an economic and scalable approach to anisotropic liquids and hydrogels making use of a novel bola-amphiphile motif consisting of alkenyl succinic ester terminated hydrophobic di- and polyester based spacer. We have shown that a remarkable degree of order can be obtained from ill-defined mesogens which are based on technical grade raw materials consisting of numerous isomers as well as a plurality in molecular weights regarding polymer comprising reaction mixtures. With regard to the latter we have shown that terminal hydrophobic side groups stabilize assemblies formed from species of different molecular weight and size. Such anisotropic nanosized objects display nematic or lamellar like ordering depending on the length of the terminal side chains.

Monomeric diester bola-amphiphiles from C8 to C12 alkenyl succinic ester attached to hydrogenated bisphenol-A as rigid spacer yield ordered dispersions. Such hydrogels form over the most extended concentration and temperature range in the case of C8 side chains. These phases can best be understood as polymorphism between porous lamellae (mesh) and a L_3 sponge phase. The plurality of isomeric species with different shape and aliphatic chain position allows for the allocation of different curvatures of the water organic interface, thus leading to scale invariance and nearly constant elastic response to external force. Longer as well as bulkier groups narrow the concentration range for the ordered phases and, in the case of branched chains, their temperature stability.

It will be the matter of further studies to unravel in more detail the mesogen behaviour of individual isomers of the ASA-HBA family with regard to the spacer as well as the different side groups.

Regarding both the economic and sustainable feedstock with respect to alkenyl succinic anhydrides and dimer fatty acid as well as the simple synthesis and manufacturing processes, and taking into account comparatively low amounts of polar groups, the authors anticipate that the presented polymer based approach will pave the way for ordered liquids as a formulation basis in the development of anisotropic materials for large scale applications like functional films, coatings or adhesives. Thus it is conceivable to make use of surface induced ordering effects – be it macroscopic or internal ones like layered nano particles, process related small shear flow or intrinsically replicating order phenomena in passing through the systems phase diagram in the course of water evaporation.

However careful validation of technical grade raw materials and possibly adaptation of process parameter in the course of the scale-up procedure are required for the sake of quality control.

Acknowledgements

The authors would like to thank Svetlana Guriyanova[1] (cryo-AFM), Volodymyr Boyko[1] (SAXS), Thomas Frechen[1] (cryo-TEM, SEM), Elke Austrup[2] (PES synthesis), Martina Moellers[2] (PLM), Klaus Brockkötter[2] (^{2}H-NMR), Julia Uckelmann[2] (rheology), Alex Oliver[3] and Charl Faul[3] (starting from PES, 1st trials to synthesize and to disperse the systems **3a**, **3d**, **3h,** in the frame of a summer project in 2011), Reinhard Doetzer[1] for fruitful discussions in the context of HBA isomer assignment.

[1] BASF SE
[2] BASF Coatings GmbH
[3] School of Chemistry, University of Bristol

Notes and references

[a] *BASF Coatings GmbH, Glasuritstrasse 1, 48165 Muenster, Germany. E-mail: horst.hintze-bruening@basf.com Fax: +49 2501 1471 2007; Tel: +49 2501 140,*
[b] *University of Applied Science of Muenster, Stegerwaldstrasse 39, 48565 Steinfurt, Germany,*
[c] *BASF SE, Carl-Bosch-Strasse 38, 67063 Ludwigshafen, Germany.*

†1 Measured at 1Hz. Frequency sweeps of **4c** and **4e** (w = 0,4) as well as **4d** (w = 0,5 and 0,6) measured with an amplitude of 0,1 mrad are shown in figure S12. Between 1 and 100 Hz moduli steadily increase, the loss moduli of the hydrogels approaching the storage moduli at the high frequency end. For the viscous liquid **4d** (w = 0,5) exponentially increasing G' narrows the gap between moduli at higher frequency. The typical range of shear stress covered by the sweeps was in the range of 0,4 and 18 Pa for the hydrogels and 10 to 24 Pa for the

viscous liquid of **4d** (w = 0,5).

†2 Missing birefringence, but dried **4a** displays textures of crystals.

†3 Macroscopic the sample can easily be sliced into extended flakes.

Electronic Supplementary Information (ESI) available: [analytical data of HBA isomerism, all SAXS peak positions, ^{2}H-NMR- and rheology charts referred to in the text but not shown in the figures to keep the article manageable, calculated compositions of bola-amphiphile mixtures]. See DOI: 10.1039/b000000x/

1 Y. Wan and D. Zhao, *Chem. Rev.*, 2007, **107**, 2821; X. Zhang et.al., *Angew. Chem. Int. Ed.*, 2010, **49**, 10101; C. Rodriguez et.al., *J. Dispersion Sci. Technol.*, 2007, **28**, 1136.

2 I. Amar-Yuli et.al., *Curr. Opin. Colloid Interface Sci.*, 2009, **14**, 21; P.T. *Spicer*, *Curr. Opin. Colloid Interface Sci.*, 2005, **10**, 274; A. Angelova et.al., *Acc. Chem. Res.*, 2011, **44**, 147.

3 D.H. Thompson et.al., *Proc. SPIE, Organic and Biological Opto-electronics,* 1993, **1853**, 142; S. Laschat et.al., *Angew. Chem. Int. Ed.*, 2007, **46**, 4832.

4 T. Ikeda and O. Tsutsumi, *Science*, 1995, **268**, 1873; L. Schmidt-Mende et.al., *Science*, 2001, **293**, 1119; K. Ichimura, *Chem. Rev.* 2000, **100**, 1847.

5 A.-L. Troutier-Thuilliez et. al., *Soft Matter*, 2011, **7**, 4242.

6 R.M. Fuoss and D. Edelson, D., *J. Am. Chem. Soc.*, 1951, **73**, 269.

7 S. Yiv et.al., *J. Phys. Chem.*, 1976, **80**, 2651; Y. Okahata and T.J. Kunitake, *J. Am. Chem. Soc.*, 1979, **101**, 5231.

8 A. Gulik et.al., *J. Mol. Biol.*, 1985, **182**, 131.

9 M.A. Voronin et.al., *ACS Appl. Mater. Interfaces*, 2011, **3**, 402; J. Paczesny et.al., *Phys. Chem. Chem. Phys.*, 2012, **14**, 14365; J.K.W. Chui et.al., *Beilstein J. Org. Chem.*, 2011, **7**, 1562; N. Nuraje et. al., *Progr. Polym. Sci.*, 2013, **38**, 302.

10 K. Liu et.al., *Chem. Eur. J.*, 2012, **18**, 8622; G. Wu et.al., *Chem. Sci.* **4** (2013), 4486; P. Xing et.al., *RSC Adv*. 2013, **3**, 24776.

11 A. Polidori et.al., *ARKIVOC*, 2006, **iv**, 73.

12 J. Guilbot et.al., *Langmuir*, 2001, **17**, 613.

13 J. Wang et. al., *J. Sci. Food Agric.*, 2010, **90**, 424; P. Dokic et.al., *Progr. Colloid Polym. Sci.*, 2008, **135**, 48.

14 J.C. Roberts, *The Chemistry of Paper*. Chapter 7, *Chemical Additives in the Paper Formation Process*, pp 124-130, Royal Society of Chemsitry, Herts, UK, 1996.

15 D. Tsiourvas et.al., *Progr. Colloid Polym. Sci.*, 1994, **97**, 163.

16 J.-H. Fuhrhop et.al., *Langmuir*, 1985, **1**, 387.

17 R. Ramaswamy et.al., *J. Appl. Polym. Sci.*, 1987, **33**, 49.

18 C.Y. Zhang et.al., *Phys. Rev. E*, 1993, **48**, 2850; R. Strey and R. Schomäcker, *J. Chem. Soc. Faraday Trans.*, 1990, **86**, 2253.

19 N. Satoh and K. Tsujii, *J. Phys. Chem.*, 1987, **91**, 6629.

20 J. Cortese et.al., *J. Am. Chem. Soc.*, 2011, **133**, 19672.

21 J.-H. Fuhrhop and D. Fritsch, *Acc. Chem. Res.*, 1986, **19**, 130.

22 fig. 15 in: F.B. Rosevear, *J. Soc. Cosmetic Chemists*, 1968, **19**, 581.

23 E.O. Kiirend et.al., *Crystallography Reports* **47** (2002) 849; H. Hoffmann et.al., *Langmuir* 1994, **10**, 3972; J. Oberdisse et.al., *Langmuir* 1996, **12**, 1212.

24 S.T. Hyde, Chapter 16, pp 315, in K. Holmberg. *Handbook of Applied Surface and Colloid Chemistry*, John Wiley & Sons, 2001; A.M. Figueiredo Neto and S.R.A. Salinas, *The Physics of Lyotropic Liquid Crystals*, p 174, Oxford University Press, Oxford, 2005.

25 G. Porte et.al., J. *Phys. II*, 1991, **1**, 1101.

26 G. Porte, *J. Phys.: Condens. Matter*, 1992, **4**, 8649.

27 M.C. Holmes, Part I, Chapter 3, pp 99, in A.V. Zvelindovsky, *Nanostructured Soft Matter*, Springer, 2007.

28 J.C. Blackburn and P.K. Kilpatrick, *Langmuir*, 1992, **8**, 1679.

29 J. Charvolin and J.-F. Sadoc, *J. Phys. Chem.*, 1988, **92**, 5787.

Electronic Supplementary Information

Composition and Isomerism in Hydrogenated Bisphenol A

GC analysis of hydrated Bisphenol A, the hydroxyls silylated using N-Methyl-N-trimethylsilyl-trifluoracetamid (MSTFA), and the mass spectra for the five detected peaks. After recrystallization in chloroform GC essentially detects two components. The melting point (m.p.) of the isolated fraction was determined to be 183°C, well above reported m.p. for cis,trans (165°C) and cis,cis (175°C) and below m.p. for trans,trans (188°C).[1] We assign the two recrystallized isomers to trans,trans (91%) and cis,trans (9%). This gives an isomer composition of the neat product to be: 0,9% monool 1, 2,1% monool 2, 7,8% cis,cis-diol, 40,5% cis,trans-diol and 48,7% trans, trans-diol. This is corroborated by integrated ^{13}C signals for the methine carbons (C4, C8) at 42,93 ppm for trans,trans (49%), 43,67 and 42,61 ppm for cis,trans (two nearly identical intensities adding to 42%) and 43,34 ppm for cis,cis (9%).[2]

[1] Bull. Chem. Soc.Jpn **39** (1966) 2191
[2] assignments according ACD labs NMR predictor

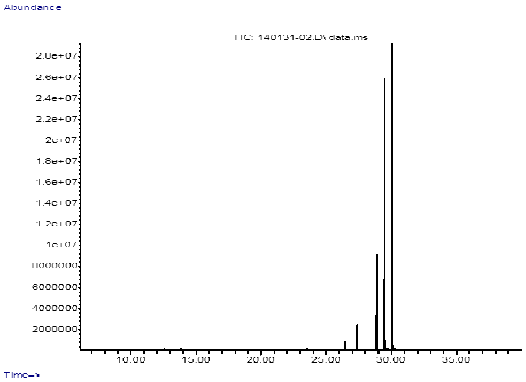

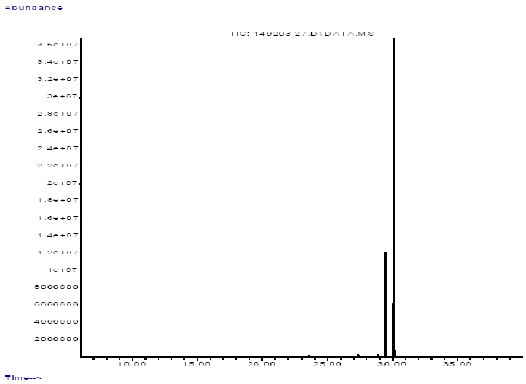

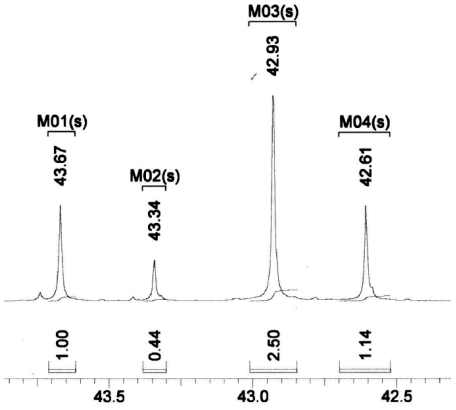

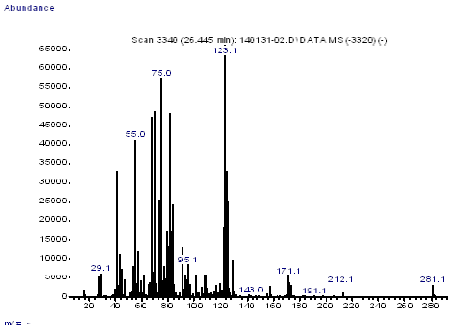

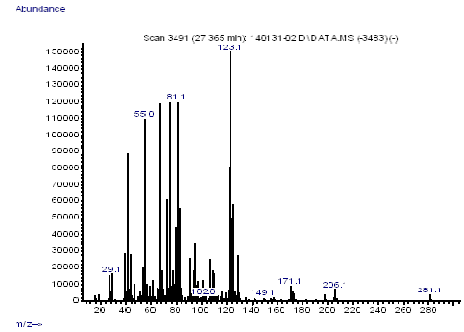

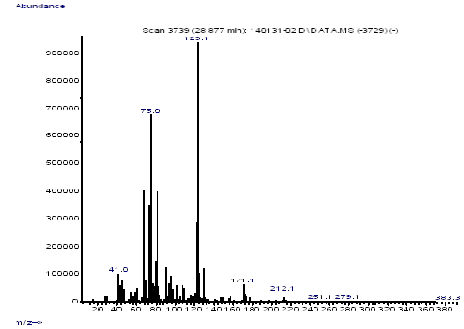

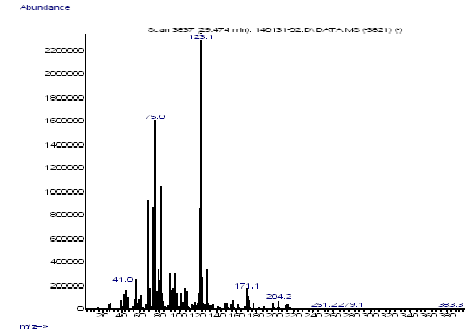

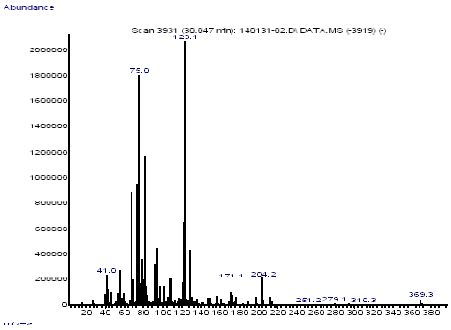

no.	HPA	DFA	HBA	ASA-C8	ester groups	MW	d [Å]
1	**0**	**0**	**1**	**2**	**2**	**662**	**21,9**
2	0	1	2	2	4	1432	57,3
3	**0**	**2**	**3**	**2**	**6**	**2201**	**94,7**
4	0	3	4	2	8	2971	132,2
5	0	4	5	2	10	3740	169,4
6	1	0	2	2	4	1039	38,1
7	**1**	**1**	**3**	**2**	**6**	**1808**	**73,7**
8	1	2	4	2	8	2578	111,6
9	1	3	5	2	10	3347	147,1
10	1	4	6	2	12	4116	187,4
11	**2**	**0**	**3**	**2**	**6**	**1415**	**52,8**
12	2	1	4	2	8	2185	89,7
13	2	2	5	2	10	2954	128,6
14	2	3	6	2	12	3723	165,3
15	2	4	7	2	14	4493	203,1
16	3	0	4	2	8	1792	71,3
17	3	1	5	2	10	2561	108,6
18	3	2	6	2	12	3330	145,8
19	3	3	7	2	14	4100	183,1
20	3	4	8	2	16	4869	220,3
21	4	0	5	2	10	2168	86,8
22	4	1	6	2	12	2937	124,1
23	4	2	7	2	14	3707	161,3
24	4	3	8	2	16	4476	198,6
25	4	4	9	2	18	5246	235,8

Table S1 Calculated molecular weights and dimensions of theoretically formed stretched (all trans) polymers for polyester bola-amphiphile **3c**. Dimensions result from measurements using the software ChemDraw.Highlighted entries no. 3 and 11 have been considered as the prevalent species based on the assumption that esterification is kinetically controlled due to a distinct different reactivity declining from HPA (ring opening), over DFA to HPA (2nd carboxylic group) for the diacid as well as for the HBA isomers with "trans,trans" reacting faster than trans in "cis,trans" and these in turn faster than "cis,cis". Entry no. 1 reflects the excess HBA essentially consisting of the cis,cis isomer (see article).

BA	d.n.	w	q [nm^{-1}]	d [nm]	q [nm^{-1}]	d [nm]	q [nm^{-1}]	d [nm]
3h	0,75	0,58	0,374	16,8	0,681	9,2	1,367	4,6
		0,67	0,407	15,4	0,711	8,8	1,424	4,4
		0,73	0,445	14,1	0,742	8,5	1,486	4,2
		0,78	0,484	13	0,756	8,3		
3a	0,55	0,54	0,6 / 0,9	10,7 / 7				
		0,62	0,6 / 1,1	10,8 / 5,7				
		0,71	0,6 / 1,2	10,4 / 5,2				
3b	0,66	0,52	0,389	16,1				
		0,62	0,46	13,7				
		0,71	0,486	12,9				
3c	0,63	0,33	0,288	21,8	0,568	11,1		
		0,42	0,341	18,4	0,639	9,8		
		0,51			0,855	7,4		
		0,6	0,687	9,1	1,102	5,7	2,213	2,8
3e	0,68	0,31	0,226	27,8	0,539	11,6		
		0,34	0,233	27	0,597	10,5		
		0,37	0,264	23,8	0,643	9,8		
		0,43	0,297	21,2	0,734	8,6		
		0,47			0,82	7,7		
3f	0,7	0,37	0,255	24,7	0,65	9,7		
		0,49			0,789	8		
		0,59			0,959	6,6		
3g	0,59	0,36	0,422	14,9				
		0,4	0,372	16,9				
		0,5	0,365	17,2	0,462	13,6		
		0,6	0,442	14,2	0,544	11,6		

Table S2 SAXS data obtained on aqueous dispersions of polymeric bola-amphiphiles at given concentrations (w) at 20°C. The degree of neutralization (d.n.) indicates the fraction of carboxylic acid groups neutralized with dimethyl ethanol amine after the distillation step to remove the solvent (see experimental part). Scattering vector (q) values and corresponding distances in real space (d) refer to the humps (left), the 1st harmonic peaks (center) and 2nd harmonic peaks (right) of the scattering curves.

ASA alkenyl C=C bond isomers	
	w_i
cis	0,2
trans	0,8

R1 position relative to ester group	
	w_i
alpha	0,38
beta	0,62

R1 position and ring configuration	
	w_i
alpha-eq	0,26
alpha-ax	0,12
beta-eq	0,45
beta-ax	0,17

hydroxyl ring configuration (diol only)		
renormalized	w_i	
eq-eq	0,50	*trans,trans*
eq-ax	0,42	*trans,cis*
ax-ax	0,08	*cis,cis*

end group isomers		
		w_i
CAE	cis-alpha-eq	0,052
CAA	cis-alpha-ax	0,024
CBE	cis-beta-eq	0,090
CBA	cis-beta-ax	0,034
TAE	trans-alpha-eq	0,208
TAA	trans-alpha-ax	0,096
TBE	trans-beta-eq	0,360
TBA	trans-beta-ax	0,136

CAE = cis, alpha, equatorial
TBA = trans, beta, axial

4c Isomer		w_i	molecules	round	used
TBE	TBE	0,2173	7,387	7	8
TAE	TBE	0,1255	4,268	4	5
TBE	TBA	0,0821	2,791	3	4
TAE	TAE	0,0725	2,466	2	3
TAA	TBE	0,0579	1,970	2	2
CBE	TBA	0,0543	1,847	2	2
TAE	TBA	0,0474	1,612	2	2
TAE	TAA	0,0335	1,138	1	1
CAE	TBE	0,0314	1,067	1	1
CBE	TAA	0,0314	1,067	1	1
TBA	TBA	0,0310	1,054	1	1
TAA	TBA	0,0219	0,744	1	1
CBA	TBE	0,0205	0,698	1	1
CAE	TAE	0,0181	0,617	1	1
TAA	TAA	0,0155	0,525	1	1
CAA	TBE	0,0145		30	34
CBE	TBE	0,0145			
CBE	CBA	0,0136			
CAE	TBA	0,0119			
CBA	TAE	0,0119			
CAE	TAA	0,0084			
CAA	TAE	0,0084			
CAE	CBE	0,0078			
CBA	TBA	0,0078			
CAA	TBA	0,0055			
CBA	TAA	0,0055			
CBE	TAE	0,0051			
CAE	CAE	0,0045			
CAA	TAA	0,0039			
CAA	CBE	0,0036			
CBE	CBE	0,0036			
CAE	CBA	0,0030			
CAE	CAA	0,0021			
CBA	CBA	0,0019			
CAA	CBA	0,0014			
CAA	CAA	0,0010			

Table S3 List of isomers found on the basis of GC analysis on **2c** and HBA as well as NMR analysis of HBA and the reaction product **4c** (left). Results for R1 position and ring positions comprise ALL HBA isomers, the monool included. However the hydroxyl ring configuration for the latter was renormalized to the diol fraction and used for the calculation of the isomers of **4c** assuming independent probability for the two sides of the spacer diol. The products are listed with their decreasing percentage in the mixture (centre). For the simulation of a given box-size of 16.000 atoms 34 molecules of 4c are needed. These were arbitrarily restricted to the most abundant isomers (wi > 0,015). The four missing molecules were then added to the four most frequent isomers (right).

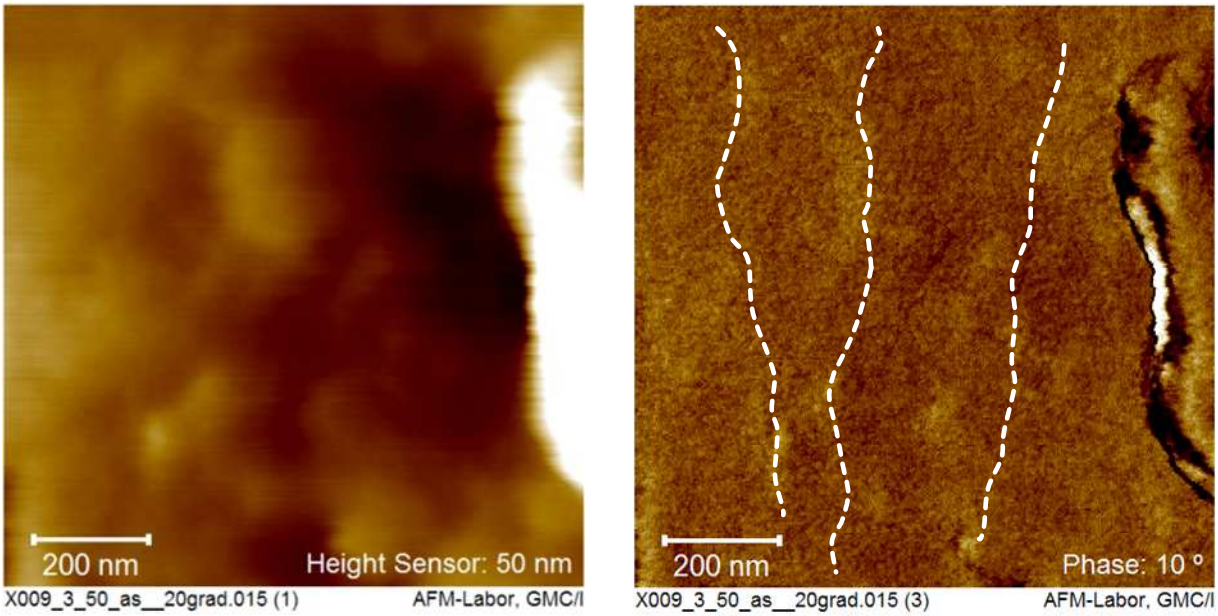

Fig. S1 cryo-AFM imaging of **3f** (w = 0,49) frozen at 0°C shows nematic alignment of nano sized anisotropic objects in the phase contrast (right image). Dashed white lines in the phase contrast image (right) designate the local alignment as guidance for the eyes.

q values	w	4c	4d	4e
	0,3	0,91	1,2	0,80
	0,4	1,25	1,3	1,11
	0,5	1,61	1,4	1,43
	0,6	1,93	1,59	1,69
	0,7	2,18	1,79	2,0
d [nm]	**w**	**4c**	**4d**	**4e**
	0,3	6,88	5,37	7,82
	0,4	5,03	4,97	5,66
	0,5	3,91	4,45	4,39
	0,6	3,26	3,94	3,72
	0,7	2,88	3,51	3,22
			C12 - C8	C12 br - lin
Δd	**w**	**4d - 4c**	**4e - 4c**	**4e - 4d**
	0,3	**-1,51**	**0,94**	**2,45**
	0,4	**-0,06**	**0,62**	**0,69**
	0,5	**0,55**	**0,49**	**-0,06**
	0,6	**0,69**	**0,46**	**-0,23**
	0,7	**0,63**	**0,34**	**-0,29**

Table S4 Peak and hump maxima (highlighted in red) positions q [nm^{-1}] of first harmonics of the amphiphiles **4c**, **4d** and **4e** for the concentrations 0,3 > w < 0,7 at 20°C, their corresponding distances d [nm] and the difference between phases with same w values of **4c** and **4d**, **4c** and **4e** and **4d** and **4e** respectively.

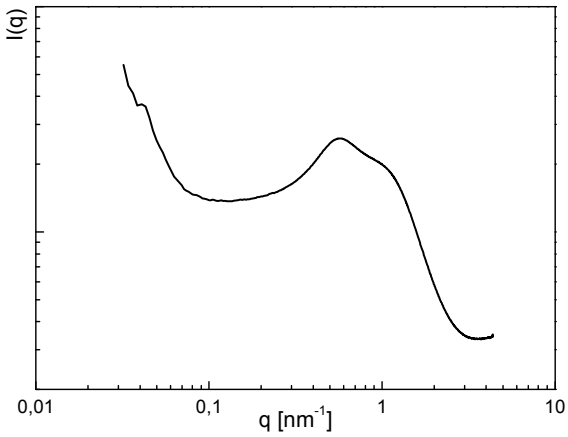

Fig. S2 USAXS on an aqueous dispersion of polymeric BA **3a** (w = 0,62) at 20°C. A broad peak around q = 0,042 corresponds to swollen lamellae (d ~ 150 nm). Broad humps are attributed to an isotropic, non ordered phase of dissolved bola-amphiphile species.

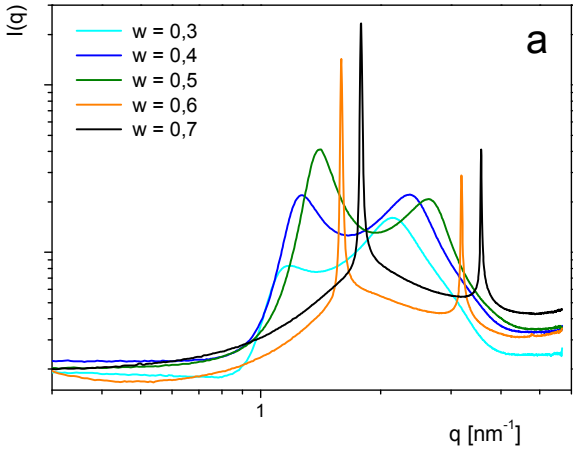

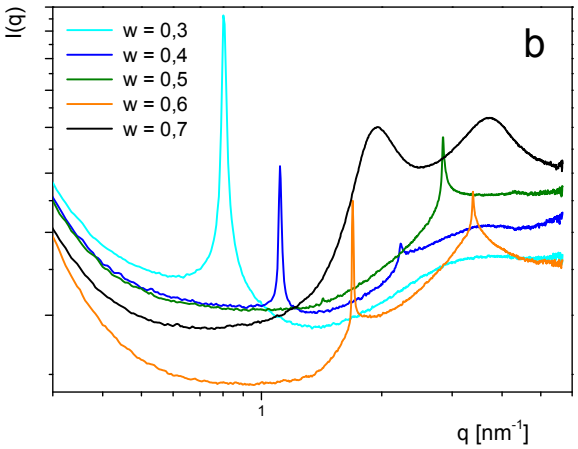

Fig. S3 SAXS curves from phases of (a) **4d** and (b) **4e** at concentrations 0,3 < w > 0,7 at 20°C. Peaks, or humps maxima respectively, shift to higher q values with increasing w.

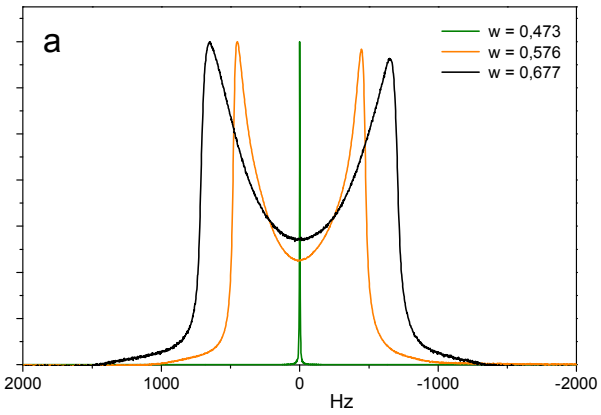

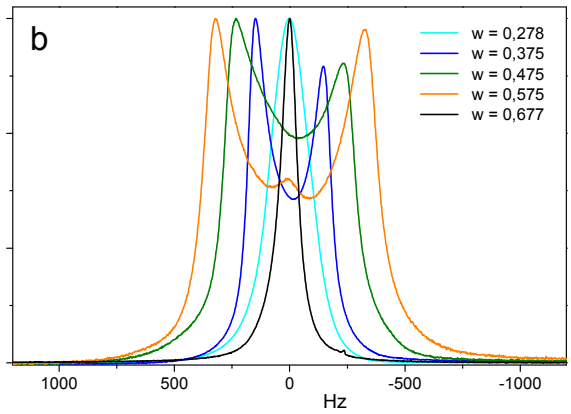

Fig. S4 ^{2}H-NMR quadrupole splittings for aqueous dispersions of (a) **4d** and (b) **4e** at concentrations 0,5 < w > 0,7 and 0,3 < w > 0,7 respectively at 20°C. Lower concentrations of **4d** yield signals identical to w = 0,5.

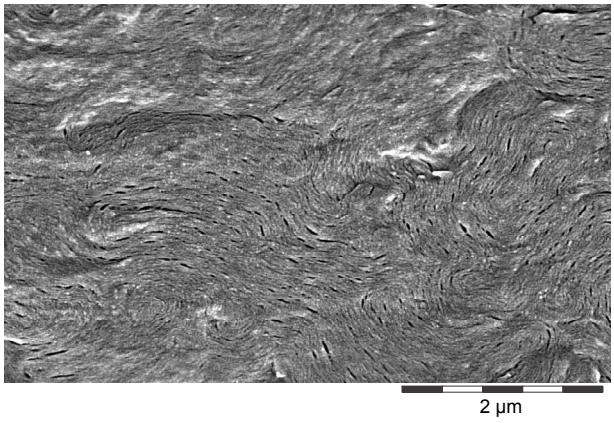

Fig. S5 cryo-SEM image of **4e** (w = 0,5) showing the lamellar like texture comprising bended domains on the nano- to microscale.

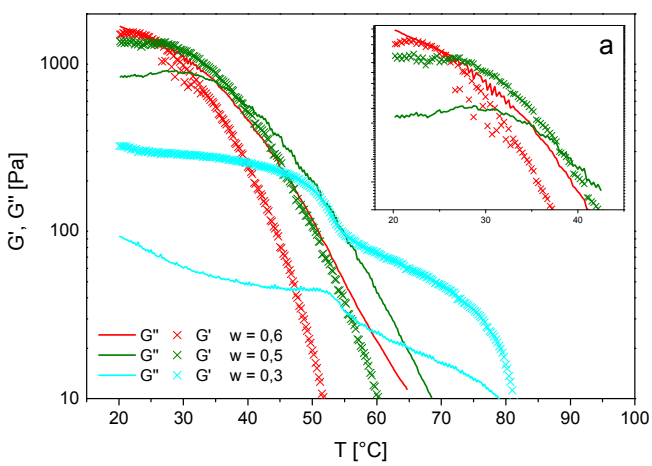

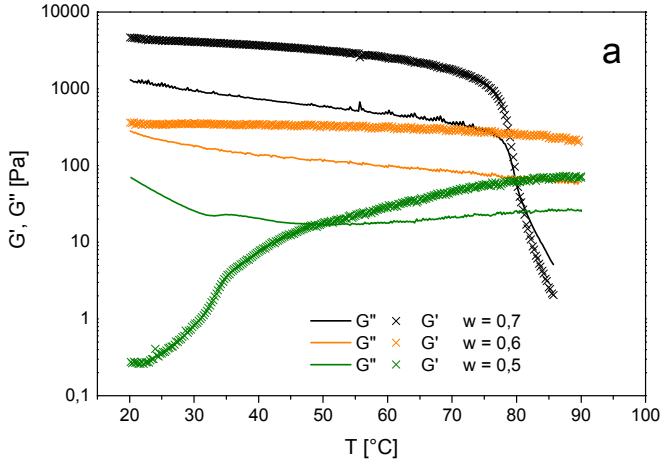

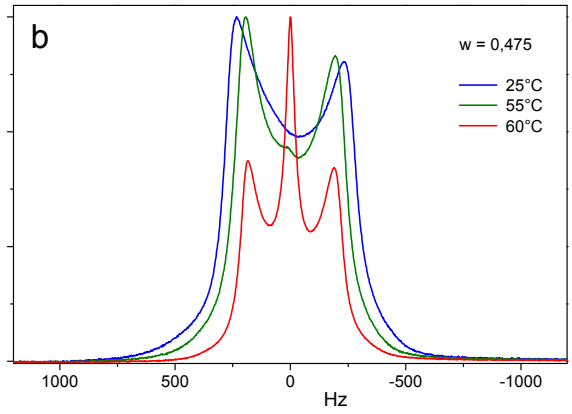

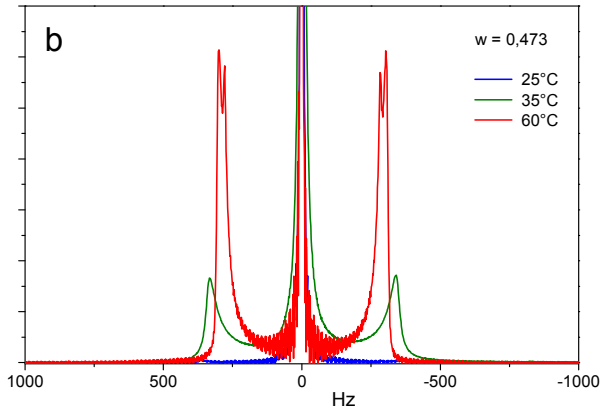

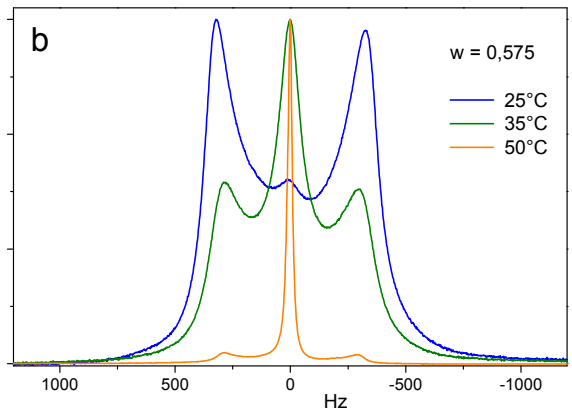

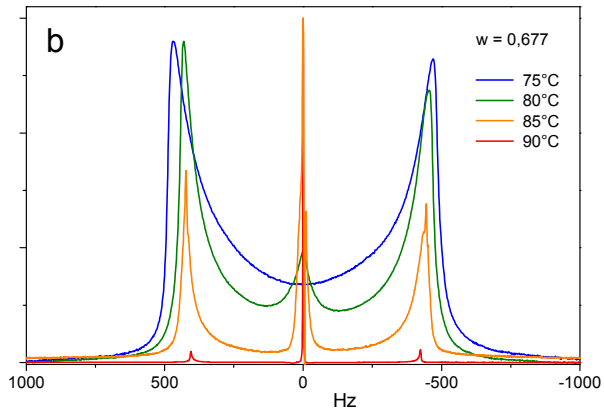

Fig. S6 (a) Temperature dependancy of storage (G', crosses) and loss moduli (G'', lines) of **4e** dispersions at concentrations w = 0,3, 05 and 0,6 (the insert showing a magnified section for the latter), (b upper chart) ^{2}H-NMR curves for the phase at w = 0,5 at 25°C, 55°C and 60°C and (b lower chart) ^{2}H-NMR curves for the phase at w = 0,6 at 25°C, 35°C and 50°C. Decline and crossing of the moduli G' and G'' of these phases are reflected by an increasing fraction of an isotropic phase within these dispersions.

Fig. S7 (a) Temperature dependancy of storage (G', crosses) and loss moduli (G'', lines) of **4d** dispersions at concentrations w = 0,5, 06 and 0,7, (b upper chart) ^{2}H-NMR curves for the phase at w = 0,5 at 25°C, 35°C and 60°C (n.b. intensity on y-axis: scale factor is 22 times the scale of all other 2H-NMR charts, compare w = 0,5 25°C with fig. S3a!) and (b lower chart) ^{2}H-NMR curves for the phase at w = 0,7 at 75°C, 80°C, 85°C and 90°C. At w = 0,5 heating leads to minor proportions of different anisotropic phases coincidating with a step in G' and a crossover of G' and G'' respectively. At w = 0,7 decline and crossing of the moduli G' and G'' around 80°C are reflected by the formation of an isotropic phase wich dominates at 90°C.

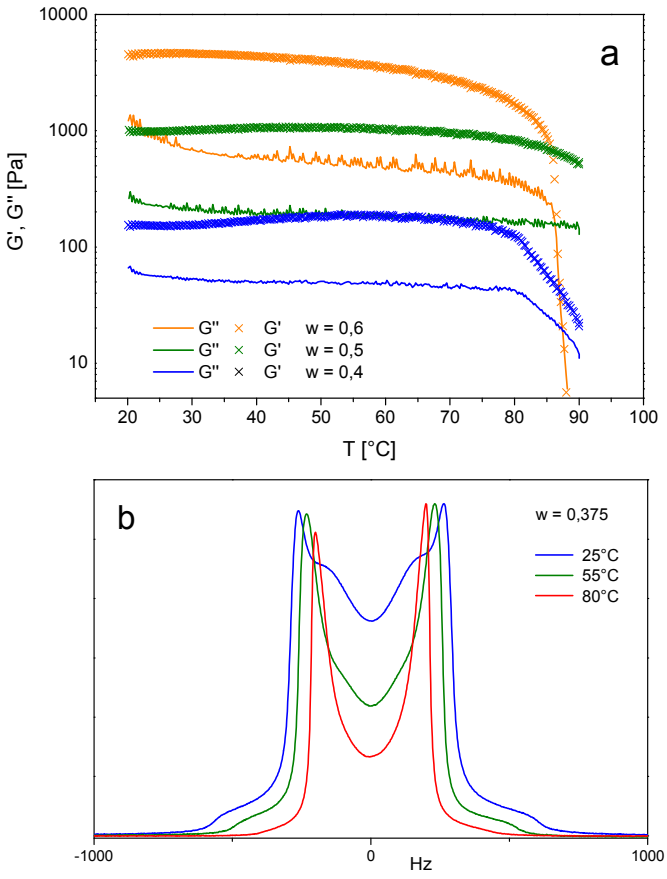

Fig. S8 (a) Temperature dependancy of storage (G', crosses) and loss moduli (G'', lines) of **4c** dispersions at concentrations w = 0,4, 05 and 0,6, (b) ^{2}H-NMR curves for the phase at w = 0,4 at 25°C, 55°C and 80°C showing that two anisotropic phases merge into one around 60°C.

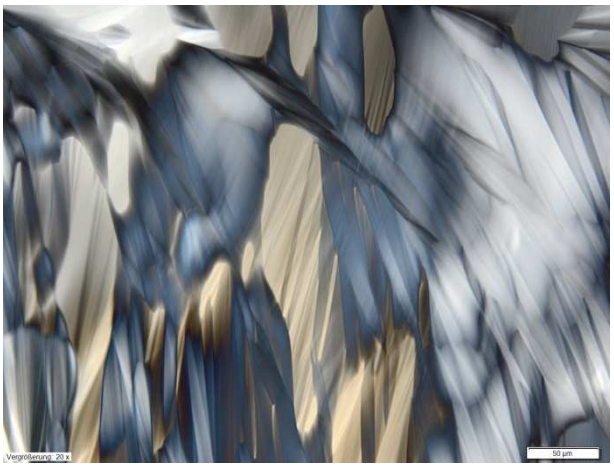

Fig. S9 OPM image showing the fan like texture of a hexagonal phase of hydrolyzed **2c** after neutralization with dimethylethanol amine in water (w = 0,67) at ambient temperature (scale bar is 50 µm).

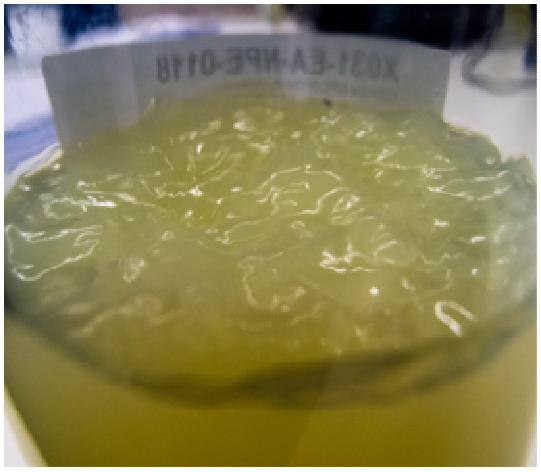

Fig. S10 Photograph showing the mesophase of **PES-NB** (w = 0,35) after 26 month storage at ambient conditions.

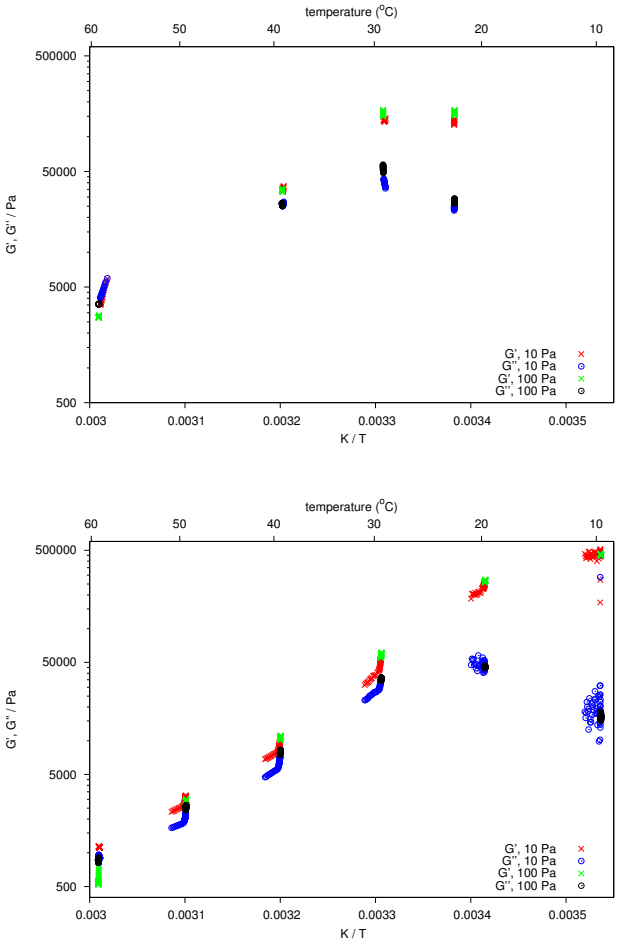

Fig. S11 Development of storgae (G') and loss modulus (G'') of the aqueous dispersion of PES-NB at w = 0,35 as a function of temperature (a) heating of a freshly applied sample (elastic solid) and (b) cooling of a molten (liquid) sample.

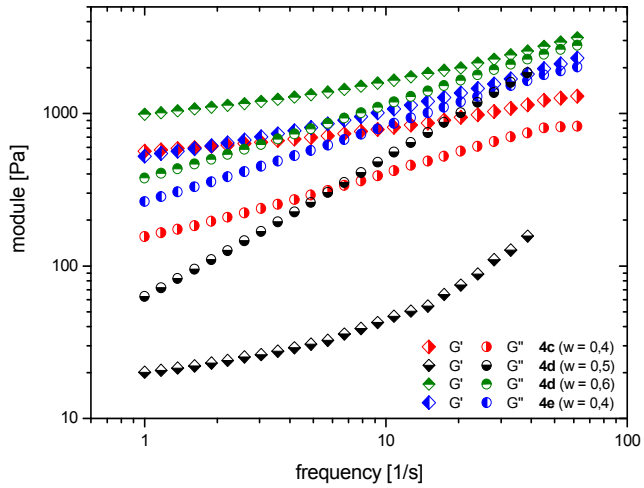

Fig. S12 Frequency sweeps of the hydrogels of **4c** and **4e** (w = 0,4) and **4d** (w = 0,6) as well as the viscous liquid of **4d** (w = 0,5) showing an increase of storage (G', losange) and loss (G'', circles) moduli with increasing frequency.

An economic and scalable route to ordered liquids and hydrogels based on novel and ill-defined, alkenyl succinic ester terminated bola-amphiphiles.